Too Much of a Good Thing: The Unique and Repeated Paths Toward Copper Adaptation

Aleeza C. Gerstein,[1,2] Jasmine Ono,[1] Dara S. Lo,[3] Marcus L. Campbell, Anastasia Kuzmin, and Sarah P. Otto[4]
Department of Zoology and Biodiversity Research Centre, University of British Columbia, Vancouver, British Columbia, Canada, V6T 1Z4

ABSTRACT Copper is a micronutrient essential for growth due to its role as a cofactor in enzymes involved in respiration, defense against oxidative damage, and iron uptake. Yet too much of a good thing can be lethal, and yeast cells typically do not have tolerance to copper levels much beyond the concentration in their ancestral environment. Here, we report a short-term evolutionary study of *Saccharomyces cerevisiae* exposed to levels of copper sulfate that are inhibitory to the initial strain. We isolated and identified adaptive mutations soon after they arose, reducing the number of neutral mutations, to determine the first genetic steps that yeast take when adapting to copper. We analyzed 34 such strains through whole-genome sequencing and by assaying fitness within different environments; we also isolated a subset of mutations through tetrad analysis of four lines. We identified a multilayered evolutionary response. In total, 57 single base-pair mutations were identified across the 34 lines. In addition, gene amplification of the copper metallothionein protein, *CUP1-1*, was rampant, as was chromosomal aneuploidy. Four other genes received multiple, independent mutations in different lines (the vacuolar transporter genes *VTC1* and *VTC4*; the plasma membrane H+-ATPase *PMA1*; and *MAM3*, a protein required for normal mitochondrial morphology). Analyses indicated that mutations in all four genes, as well as *CUP1-1* copy number, contributed significantly to explaining variation in copper tolerance. Our study thus finds that evolution takes both common and less trodden pathways toward evolving tolerance to an essential, but highly toxic, micronutrient.

KEYWORDS *Saccharomyces cerevisiae*; genetic basis of adaptation; copper tolerance; aneuploidy; *CUP1*; fitness; parallel adaptation

IN his book, *Wonderful Life* (Gould 1989, p. 51), Stephen J. Gould famously opined that evolution is a historical and contingent process, so much so that "any replay of the tape would lead evolution down a pathway radically different from the road actually taken." While this is undoubtedly true when one considers the full complexity of an organism, refrains are often observed in evolution at the trait level. Repeated evolution, defined as "the independent appearance of similar phenotypic traits in distinct evolutionary lineages" (Gompel and Prud'homme 2009) has been documented in both ecological and clinical environments at all taxonomic levels, *e.g.*, repeated loss of stickleback lateral plates in freshwater (Schluter *et al.* 2004), ecomorphs of Anolis lizards (Losos 1992), the acquisition of "cystic fibrosis lung" phenotypes in *Pseudomonas aeruginosa* in patients with cystic fibrosis (Huse *et al.* 2010), to name but a few. The development of sequencing technologies has recently allowed biologists to ask whether parallel genetic changes underlie observations of parallel phenotypic change. In some cases, parallel phenotypic evolution has been attributed to parallel genotypic evolution, for example, repeated changes to *cis*-regulatory regions of the same gene—the pigmentation gene *yellow*—underlie changes in wing pigmentation in male *Drosophila* (Prud'homme *et al.* 2006). At the other extreme are cases where different genetic targets underlie similar phenotypic shifts; for example, yeast adapting to rich media converged in fitness via a variety of genetic mechanisms (Kryazhimskiy *et al.* 2014), and beach mice adapting to sandy coastal dunes from the Gulf and Atlantic coasts of Florida converged in coat coloration via different mutations (Manceau *et al.* 2010). In such cases, unique evolutionary trajectories at the genetic level appear repeatable at the phenotypic level.

doi: 10.1534/genetics.114.171124
Manuscript received September 22, 2014; accepted for publication December 4, 2014; published Early Online December 17, 2014.
Supporting information is available online at http://www.genetics.org/lookup/suppl/doi:10.1534/genetics.114.171124/-/DC1.
Genomic fastq files have been deposited in the National Center for Biotechnology Information–Sequence Read Archive database under the accession code PRJNA261735. The remaining raw data and statistical analyses have been deposited in the Dryad Digital Repository (http://doi.org/10.5061/dryad.5gp25).
[1]These authors contributed equally to this work.
[2]Present address: Department of Genetics, Cell Biology, and Development, University of Minnesota, Minneapolis, MN 55455.
[3]Present address: Department of Molecular Genetics, University of Toronto, Toronto, ON, Canada M5S 3E1.
[4]Corresponding author: University of British Columbia, 6270 University Blvd., Vancouver, BC V6T 1Z4, Canada. E-mail: otto@zoology.ubc.ca

The degree of phenotypic repeatability is inherently linked with the genomic target size of appropriate mutations, with single-locus Mendelian traits with fewer target sites (and hence higher repeatability) at one extreme and quantitative traits at the other extreme. Even when multiple genes underlie a selected trait, however, there may be relatively few sites that, when mutated, have the magnitude of effect and sufficiently minor deleterious side effects to improve fitness overall (Stern 2013). Such pleiotropic constraints are thought to explain why *cis*-regulatory sites more often contribute to adaptation than *trans*-regulatory changes (Stern 2000; Gompel *et al.* 2005). The size of the population and the manner in which it reproduces are also critical. Large populations have access to rarer mutations, particularly those of large effect (Burch and Chao 1999), increasing the chance that the best of these mutations will fix in independent evolutionary trials (Bell and Collins 2008). Mutations with particularly high fitness are also more likely to fix in asexual populations, because clonal interference reduces the chance that minor-effect mutations establish (Rozen *et al.* 2002), unless adaptive mutations are so common that coalitions of mutations establish together (Fogle *et al.* 2008; Lang *et al.* 2013).

The nature and severity of environmental challenge will also affect the degree of repeatability at both the genotypic and phenotypic levels. If the environmental change is so severe that the population cannot replace itself and there are only a small fraction of mutations whose benefits are large enough to bring absolute fitness above one (Bell and Collins 2008), then adaptation would be more repeatable. On the other hand, if an organism is adapting via mutations whose effects are small relative to the distance to the fitness optimum, nearly half of mutations are predicted to be beneficial (Fisher 1930), and adaptation would be less repeatable. The genomic target size must also depend on the nature of mutations required: when adaptation can be accomplished by the loss of a function, adaptive mutations can potentially arise in any step along the pathway leading to that function via a variety of mechanisms [*e.g.*, single base-pair changes leading to premature stop codons early within a gene, movement of transposable elements within a gene, mutations in the promoter that alter transcription factor (TF) binding sites, etc.]. In contrast, if the environmental challenge requires the appearance of a novel trait, or an alteration of an existing trait, the number of genomic targets is likely diminished. Despite these long-standing theoretical predictions, empirical data have only recently been catching up, largely due to breakthroughs in sequencing technology (*e.g.*, Schneeberger 2014).

In this study, we set out to determine the repeatability of adaptive evolution at the genotypic and phenotypic levels using short-term experiments with the yeast, *Saccharomyces cerevisiae*. We purposefully employed a short-term experimental design in an attempt to avoid the potential influence of epistasis limiting the mutations that are sampled (Chou *et al.* 2011; Kvitek and Sherlock 2011). The design of the experiment was similar to a previous study in our group where we examined adaptation to the fungicide nystatin (Gerstein *et al.* 2012). In both cases, multiple isogenic lines of yeast were exposed to inhibitory levels of either nystatin or copper, with levels chosen to be slightly higher than those in which growth occurred reliably. Lines that showed growth were isolated and analyzed. Through whole-genome sequencing of 35 lines that evolved tolerance in the nystatin experiment, we found that adaptation repeatedly involved the same four genes in a single pathway leading to the production of ergosterol (Gerstein *et al.* 2012), the membrane-bound target of nystatin (Woods 1971). Indeed, of the 20 unique mutations identified, 18 involved the same two genes (11 different sites in *ERG3* and 7 in *ERG6*). In hindsight, the highly repeated nature of this adaptation may well be explained by the narrowness of the environmental challenge: the cells can survive by blocking the production of ergosterol, and this can be accomplished through loss-of-function mutations in the ergosterol biosynthesis pathway (particularly in *ERG3* or *ERG6*). We thus set out to assess the degree of repeatability in the face of an entirely different environmental challenge: high copper concentrations, where loss-of-function mutations are less expected.

Copper is a micronutrient that is essential for several different enzymatic processes in yeast (cytochrome oxidase involved in respiration, superoxide dismutase involved in defense against oxidative damage, and the Fet3p ferro-oxidase involved in iron uptake, Graden and Winge 1997). Thus, unlike nystatin, cells cannot entirely block copper uptake. On the other hand, copper is extremely toxic at high concentrations, both because it displaces other metal cofactors from proteins and because it produces highly reactive oxygen species, including damaging hydroxyl radicals (Peña *et al.* 1999). The fact that multiple cellular processes require copper, that multiple cellular compartments are involved in copper sequestration (especially vacuoles and mitochondria), and that multiple processes are impacted negatively by copper (Peña *et al.* 1999) suggests that adaptation to high copper concentrations may occur through a variety of mechanisms. Here we report the results of a short-term adaptation experiment to this toxic but essential metal. Through whole-genome sequencing, we identify the nature of the genetic changes that underlay the evolutionary rescue of 34 lines of *S. cerevisiae* exposed to inhibitory copper concentrations.

Materials and Methods

Evolution of haploid mutation lines

Mutations were acquired in haploid lines of the common lab strain, BY4741 (*MAT***a** *his3*Δ*1 leu2*Δ*0 met15*Δ*0 ura3*Δ*0*), obtained from Open Biosystems in 2009. Preliminary experiments determined that BY4741 grown in liquid YPD + 12.5 mM $CuSO_4$ does not show consistent growth. Instead, some populations begin growing at different times, a stochastic pattern of growth we have previously shown to be consistent with beneficial mutations in other environments (Gerstein *et al.* 2012). To initiate mutation acquisition, we streaked

BY4741 from frozen onto a YPD plate and randomly chose a single colony to grow overnight in 10 ml YPD, shaking at 30°. We added 4.5 ml of this common wild-type stock to 185.5 ml YPD + 12.5 mM $CuSO_4$ (hereafter referred to as "copper12" medium). We placed 1- ml aliquots into 180 inner wells of three 96 deep-well boxes, with 1 ml of dH_2O in the outer wells. Boxes were maintained shaking on a platform shaker at 30°. All boxes were checked daily by visual examination of the bottom of the wells. Growth was recorded when we saw precipitate on the bottom of a well and was first observed after 7 days of incubation (Supporting Information, Table S1). Twenty-four hours after growth was first seen, we manually mixed the well and froze 500 μl of culture in 15% glycerol. In this way we isolated 56 "putative mutation lines" within 14 days, postinoculation.

At the end of the mutation-accumulation phase, we struck each putative mutation line from the freezer stock onto a single YPD plate and grew them at 30°. Two of the putative mutation lines did not grow within 72 hr and were excluded from this point forward. Fourteen lines exhibited very small colonies, typical of petite colonies that have lost mitochondrial function. One of our initial goals in acquiring these mutation lines was to measure their fitness in heterozygous form; to avoid assaying nonnuclear mutations, these lines were also excluded from the set of lines we genotyped and phenotyped. From each remaining line we haphazardly chose eight colonies and inoculated each colony into 1 ml copper12 medium and 1 ml YPD (by using the same pipette tip) and incubated them at 30° with shaking. In six cases, none of the eight colonies grew in copper12 medium within 72 hr, leaving us with 34 copper-adapted mutation lines [copper beneficial mutation (CBM) lines, Table 1]. From the paired YPD culture descended from the same colony (limiting exposure of our stocks to copper), 500 μl was added to 500 μl 30% glycerol and frozen.

Sequencing of haploid mutation lines

Freezer culture from each CBM line was streaked onto YPD plates and grown for 48 hr at 30°. We haphazardly picked a single colony for each line and grew it for 24 hr in 50 ml of YPD at 30° with shaking. Genomic DNA was extracted using standard protocols (Sambrook and Russell 2001). Protocols supplied by Illumina were followed to create barcoded libraries for each line (2011 Illumina, all rights reserved). We sequenced 100-bp single-end fragments for each line, pooling 12 uniquely barcoded strains in each lane on an Illumina HiSeq 2000. Twelve samples were rerun to obtain sufficient depth of coverage using 100-bp paired-end fragments: CBM18, 20, 21, 22, 24, 25, 26, 29, 30, 34, 36, and 44.

The resulting genomic sequence data were processed using Illumina's CASAVA-1.8.0 as in Gerstein *et al.* (2012). We called SNPs and small insertions and deletions using configure-Build.pl and parsed the output files with custom UNIX and perl scripts. We took advantage of Illumina data from the previous set of experiments with nystatin (Gerstein *et al.* 2012), which were initiated from the same BY4741 culture, to determine the mutations that are common to our strain background yet different from the S288C reference genome (scergenome.fasta release R64-1-1 downloaded from the *Saccharomyces* Genome Database (SGD), http://downloads.yeastgenome.org/sequence/S288C_reference/genome_releases/); all such common mutations were removed from the dataset. Given that our lines were haploid, mutations called as heterozygous were discarded (likely alignment errors), as were SNP and indel calls of low quality ($Q < 20$). Remaining variants were checked in the alignments, using tview in samtools 0.1.7a (Li *et al.* 2009). SNPs were independently called using the bwa software package to perform the alignment along with samtools 0.1.7a to identify SNPs, using the -bq 1 option to limit data to reliable alignments (Li *et al.* 2009), confirming the set of SNPs found by CASAVA (Table 1).

To assess chromosomal aneuploidy events, the total depth of coverage for each chromosome was calculated as the proportion of sequenced sites mapping to a particular chromosome, relative to the proportion of known mapped sites located on that chromosome within the yeast reference genome (as reported by configureBuild.pl in Illumina's CASAVA 1.8.0 package).

Intergenic mutations were analyzed for gains and losses of predicted TF binding sites using Cis-BP, a new tool offered by the online Catalog of Direct and Inferred Sequence Binding Preferences (available at http://cisbp.ccbr.utoronto.ca/TFTools.php). Cis-BP compares two sequences (*i.e.*, one wild type and one mutant allele) for differential transcription factor binding inferred based on the relationship between similarity in DNA binding domain amino acid sequence and DNA sequence preferences (Weirauch *et al.* 2014).

Expected frequency of mutations causing nonsynonymous and stop codons

The expected frequency of mutations that would generate a particular type of amino acid change (synonymous, nonsynonymous, or stop) was calculated from the observed codon frequency in *S. cerevisiae* [http://downloads.yeastgenome.org/unpublished_data/codon/ysc.orf.cod; produced by J. Michael Cherry based on the 6216 ORFs within SGD as of January 1999]. For each position in each codon, the frequency of all possible mutations was calculated according to the observed spectrum of mutations reported by Lynch *et al.* (2008) based on previous studies in yeast. (Similar results were obtained using other mutation spectra, including a uniform distribution, the spectrum observed by Lynch *et al.* (2008) in their mutation-accumulation study, and the observed mutation spectrum in this study.)

Summing over the whole genome, the expected frequency of mutations leading to stop codons is 5.78%. The expected frequency of nonsynonymous mutations is 73.0% among all possible codon changes or 77.6% among only the synonymous and nonsynonymous changes (excluding those going to or from a stop codon). The expected frequency of mutations causing any change to the amino acid sequence is 78.9%, which is similar to the expectation used previously (78.7%)

Table 1 Mutations identified in the CBM lines

CBM line	*CUP1* coverage	Genome position (chr.bp)	Gene	Mutation (Watson strand)	Position (from 5′ end)	Amino acid change	Exchangeability
CBM1	1.61	X.412600	*VTC4*	C > T	800	Trp > Stop	
		XI.105507	*FAS1*	G > T	4837	Val > Phe	0.207
		XVI.420661	Intergenic	A > T			
CBM2	2.00	ChrII aneuploidy					
CBM3	2.48	VII.150650	Intergenic	G > T			
		ChrII aneuploidy					
CBM4	3.26	mito.24277[a]	*COX1*[b]	1D indel (GG C/- CC)	10460	Intron	
CBM5	3.78	X.413174	*VTC4*	C > A	226	Glu > Stop	
		X.654261	Intergenic[c]	T > C			
		XIV.284255	Intergenic	T > G			
CBM6	3.69	III.100061	*BUD3*	G > A	3781	Gly > Arg	0.178
		IV.319466	*VAM6*	T > A	655	Lys > Stop	
		mito.59168	21S_RRNA	A > G	1160	Lys > Arg	0.440
		mito.69322	tRNA-Arg	C > G	34	Arg > Gly	0.251
CBM7	0.91	II.365359	*TRM7*	C > T	361	Val > Ile	0.537
		III.306327	Intergenic	G > T			
		IV.143017	YDL176W	G > T	921	Ser > Ser	
		IV.177435	*CLB3*	T > G	663	Thr > Thr	
		V.392908	*BOI2*	C > T	805	Glu > Lys	0.323
		VII.949946	*SMI1*	C > A	954	Lys > Asn	0.457
		IX.370383	Intergenic	C > G			
		XV.215888	*MAM3*	C > G	250	Gly > Arg	0.178
		ChrVIII aneuploidy					
		ChrXVI aneuploidy					
CBM11	2.46	X.413020	*VTC4*	1D indel (GG A/- AA)	380	Phe > Ser+frameshift	
		XI.566200	*CCP1*	A > G	999	Phe > Phe	
		XII.605283	Intergenic	1D indel (TT A/- AA)			
		ChrII aneuploidy					
CBM13	4.02	X.412247	*VTC4*	C > A	1153	Glu > Stop	
		X.654261	Intergenic[c]	T > C			
CBM14	2.15	XV.215018	*MAM3*	C > T	1120	Val > Ile	0.537
CBM16	0.28	VII.480836	*PMA1*	A > T	1831	Phe > Ile	0.181
		ChrII aneuploidy					
CBM17	0.98	X.412325	*VTC4*	A > G	1075	Tyr > His	0.197
		XIII.711207	*ESC1*	C > T	4075	Leu > Phe	0.336
		XIII.821262	*FCP1*	T > C	1007	Leu > Ser	0.212
		ChrVIII aneuploidy					
		ChrXVI aneuploidy					
CBM18	2.80	V.303094	*VTC1*	G > T	289	Asp > Tyr	0.227
		VII.548326	*GSC2*	C > T	63	Asp > Asp	
		XI.646464-onwards	*FLO10*[d]				
CBM20	1.82	VII.480463	*PMA1*[e]	G > T	2204	Ala > Asp	0.193
		XV.215332	*MAM3*	C > T	806	Ser > Asn	0.390
		XVI.84024	YPL247C	C > T	173	Gly > Asp	0.188
		ChrII aneuploidy					
CBM21	1.12	VII.971165	*PFK1*	G > C	2570	Pro > Arg	0.254
		X.654261	Intergenic[c]	T > C			
		ChrII aneuploidy					
		ChrIII aneuploidy					
		ChrVIII aneuploidy					
CBM22	0.78	V.302818	*VTC1*	1D indel (CA C/- CA)	13	Pro > His+frameshift	
		ChrVIII aneuploidy					
		ChrXVI aneuploidy					
CBM24	0.77	IV.805485	Intergenic	A > G			
		IV.805517	Intergenic	G > A			
CBM25	2.28	IV.527743-onwards	*ENA5*[f]				
		XI.621992	*MLP1*	G > T	2188	Glu > Stop	
CBM26	0.66	VII.480470	*PMA1*	T > G	2197	Thr > Pro	0.164
		ChrI aneuploidy					
		ChrV aneuploidy					
		ChrVIII aneuploidy					

(continued)

Table 1, *continued*

CBM line	*CUP1* coverage	Genome position (chr.bp)	Gene	Mutation (Watson strand)	Position (from 5′ end)	Amino acid change	Exchangeability
CBM29	1.08	VII.1376	Intergenic	A > C			
		VII.480463	*PMA1*[e]	G > T	2204	Ala > Asp	0.193
		XV.566240	Intergenic	G > C			
		ChrII aneuploidy					
CBM30	3.30	ChrII aneuploidy					
CBM33	2.40	VII.618173	*VHT1*	G > C	1686	Ile > Met	0.279
		VIII.321332	*SBE22*	A > T	919	Met > Leu	0.513
		X.412080	*VTC4*[g]	C > T	1320	Trp > Stop	
		mito.24277[a]	*COX1*[b]	1D indel (GG C/- CC)	10460	Intron	
CBM34	2.92	X.412080	*VTC4*[g]	C > T	1320	Trp > Stop	
		XI.364518	Intergenic	Complex 1I indel (GA > AAT)			
		mito.24277[a]	*COX1*[b]	1D indel (GG C/- CC)	10460	Intron	
CBM36	2.15	X.412080	*VTC4*[g]	C > T	1320	Trp > Stop	
		mito.24277[a]	*COX1*[b]	1D indel (GG C/- CC)	10460	Intron	
CBM37	2.04	X.412080	*VTC4*[g]	C > T	1320	Trp > Stop	
		mito.24277[a]	*COX1*[b]	1D indel (GG C/- CC)	10460	Intron	
CBM44[h]	1.39	X.412080	*VTC4*[g]	C > T	1320	Trp > Stop	
		mito.24277[a]	*COX1*[b]	1D indel (GG C/- CC)	10460	Intron	
CBM45	2.68	X.412080	*VTC4*[g]	C > T	1320	Trp > Stop	
		mito.24277[a]	*COX1*[b]	1D indel (GG C/- CC)	10460	intron	
CBM46	2.75	X.412643	*VTC4*	T > A	757	Arg > Stop	
		XI.438478	*DID4*	A > G	701	Gln > Arg	0.366
CBM47	2.34	V.302909	*VTC1*	C > A	104	Ser > Stop	
CBM49	3.14	V.438349	Intergenic	G > C			
		XII.1034221	*HMG2*	C > T	1595	Pro > Leu	0.258
		XIII.420239	Intergenic	A > C			
		XIV.265933	*GCR2*	T > A	598	Lys > Stop	
CBM51	2.50	II.444465	*FES1*	C > T	229	Asp > Asn	0.201
		IV.310552	Intergenic	A > G			
CBM53	2.88	V.180433	*PRP22*	C > T	1593	Ile > Ile	
CBM54	1.98	VII.1077964	*MAL12*	G > T	1366	Gly > Stop	
CBM55	2.25	(no mutations except to *CUP1*)					

CUP1 coverage for each line is provided in the second column and does not account for additional copies via chrVIII aneuploidy.
[a]This mutation falls in an intron of *COX1* but causes a frameshift in an overlapping predicted gene, A15_Beta.
[b]Identical *COX1* mutation observed in seven different lines.
[c]Identical intergenic mutation observed in three different lines.
[d]The alignment formed a 100% match to the beginning of *FLO10* until XI.647464, at which point the alignment switched to a perfect match to a similar region downstream, starting at XI.648031. *In silico* qPCR confirmed the absence of unique intervening sites (CACCAGCTCTTCCTGGTCGT and CACCAGCTCTTCCTGGTCGT) within the FASTQ files for CBM18 (but present in other CBM lines), indicating a deletion in this region.
[e]Identical *PMA1* mutation observed in two different lines.
[f]The alignment within this region exhibited a 100% match to the beginning of *ENA5* but switched to a 100% match to *ENA1* from approximately site IV.527743, suggesting a deletion. Because of the highly repetitive nature of this array, *in silico* qPCR was unable to uniquely identify the missing positions.
[g]Identical *VTC4* mutation observed in six different lines.
[h]CBM44 was sequenced from the original population, not the representative colony.

based on a uniform frequency of mutations (Wenger *et al.* 2011). Because mutations are biased toward transitions and away from G/C, we recommend using the estimates reported here, which are based on the greatest amount of data regarding the mutational spectrum (Lynch *et al.* 2008).

Determination of CUP1 copy number

Using samtools 0.1.7a, the alignments of all CBM lines were manually checked at genes that are known or suspected to be important for acclimation to high levels of copper in *S. cerevisiae*, with a particular focus on genes that were previously identified to be up-regulated under high levels of copper: *BSD2*, *CCC2*, *COX23*, *CTR2*, *CUP1-1*, *CUP1-2*, *CUP2*, *FET3*, *FMP23*, *GEF1*, *HAA1*, *PCA1*, *SCO1*, *SCO2*, *SLF1*, and *VMA3*. The alignments were normal for all of these genes (including 500 bp up- and downstream), except *CUP1-1* and *CUP1-2* on chromosome VIII. In this region, large gaps were consistently found spanning the duplicated copies of these genes, caused by alignment ambiguities in this tandem repeat region.

To measure *CUP1* copy number without having to rely on alignments, we carried out the bioinformatics equivalent of a qPCR analysis (*in silico* qPCR; Gerstein *et al.* 2014) by using the unix command "grep" to directly count the number of fastq fragments containing "primers" in the *CUP1* region. Specifically, we summed the number of fragments containing the 16-bp fragment from the very beginning and from the very end of *CUP1*, plus two 16-bp fragments between *CUP1-1* and

CUP1-2 (TTTCAAGAGAACATTT and GGGTGGTGAAGTAATA), searching for all four in the forward and reverse directions (*e.g.*, using "zgrep TTTCAAGAGAACATTT *fastq*"). We then repeated this *in silico* qPCR procedure for three unique genes on chromosome VIII as controls (using the first 16 bp of *DED81*, *DUR3*, and *RIX1* in both the forward and reverse directions). A BLAST search was used to confirm that these fragments aligned only to the appropriate genes (http://www.yeastgenome.org/cgi-bin/blast-sgd.pl). We also conducted this procedure with the 35 BMN lines isolated in nystatin ["beneficial mutation nystatin"; Gerstein *et al.* (2012)], which we initiated from the same ancestral genetic background, providing a baseline for comparison. Relative to the three control genes, the BMN lines had an average of 18.13 copies of *CUP1* (range: 12.40–30.45). Note that although the S288C reference genome on the SGD reports only two *CUP1* copies, an isolate of S288C was recently found to contain ~14 copies by Southern analysis (Zhao *et al.* 2014). Our data are thus consistent with our ancestral BY4741 strain having undergone amplification in this region, and we report the number of *CUP1* copies in our copper adaptation strains relative to the average across the BMN lines.

To test whether levels of *CUP1* inferred from *in silico* qPCR were consistent with levels of *CUP1* transcription, we assayed RNA levels using quantitative real-time PCR (qPCR). Detailed methods are provided in File S1. Briefly, we chose 10 CBM lines that spanned the range of *CUP1* copy number. A single colony of each CBM line and two colonies of BY4741 were inoculated into 1 ml YPD + 5.5 mM $CuSO_4$ (a lower concentration was used to allow growth of all lines, including BY4741) and grown for 12 hr at 30° with shaking, at which point RNA was isolated using the RNEasy Mini kit from Qiagen, following the yeast protocol. Oligonucleotides for qPCR (Table 2) were designed using Primer Express (ABI). mRNA levels of *TAF10* were used for normalization, because *TAF10* exhibits stable expression across strains and conditions (Teste *et al.* 2009).

Phenotypic assays of CBM lines

To determine the extent of copper tolerance acquired, we conducted dose–response experiments in deep-well boxes. Each CBM line was struck from frozen onto YPD and grown for 48 hr at 30°. A single colony was then haphazardly chosen from each line and inoculated into 10 ml YPD, shaking overnight at 30°. The optical density of all lines was standardized to the least dense line and 200 μl of standardized culture was added to 400 μl YPD; 15μl was then inoculated into 1 ml of eight different levels of YPD + $CuSO_4$ (0 mM, 4 mM, 8 mM, 9 mM, 10 mM, 11 mM, 12 mM, and 14 mM). Four replicates were grown for each line in each level of copper. Boxes were maintained shaking on a bench top shaker at 30°. After 72 hr, we manually mixed each well and the optical density (OD) of 200 μl of culture was measured on a BioTek plate reader. With these data, we determined the IC_{50} (half-maximal inhibitory concentration) of copper using a maximum likelihood fitting procedure, as previously described (Gerstein *et al.* 2012).

Table 2 Oligonucleotides employed for RT-PCR, Southern blot analysis, and genotyping in the forward and reverse directions

Primer name	Sequence	Experiment
CUP1-F	AGCTGCAAAAATAATGAACAATGC	RT
CUP1-R	GCATTTGTCGTCGCTGTTACA	RT
TAF10-F	AAGTTGTTCTGACGGTGAACGA	RT
TAF10-R	GCGACCTATATTGAGCCCGTATT	RT
CUP1-F	5Biosg/TTAATTAACTTCCAAAATGAAGGTCA	SB
CUP1-R	5Biosg/AGACTATTCGTTTCATTTCCCAGAG	SB
MAM3-F	AATGAGTGCCGATACCATCC	GT
MAM3-R	GATTCGTCCCAATCTTTTGC	GT
VTC4-F	GTTCATGATCTAGCAAAGTTTTCG	GT
VTC4-R	GGTAACCAAAATGGGATTGAA	GT
LYS2-F	TCAAGGGCTGAAAAGACAATCAA	GT
LYS2-R	CGACGCAAAGAGATGAAACCA	GT

RT, real-time PCR; SB, Southern blot; GT, genotyping; F, forward; R, reverse.

To assess whether there was a correlation between the ability to grow in elevated levels of copper and fitness in other environments, we conducted a series of growth rate experiments using the Bioscreen C Microbiological Workstation (Thermo Labsystems) to automate OD readings. From the rise in OD, growth rates were estimated under multiple environmental conditions: YPD + 8 mM $CuSO_4$ ("copper8"); YPD, a standard laboratory rich medium; YPG, a medium that requires yeast cells to respire; and YPD + iron (ferric citrate). The latter environment was of particular interest because of copper's role in iron uptake via the Fet3p ferro-oxidase, so growth was assayed at three levels of ferric citrate: 10 mM, 40 mM, and 60 mM; we only present the 40 mM results in the main text because results were highly correlated across the iron concentrations (Table S2). Copper (0.2 M Cu(II) $SO_4 \cdot 5H_2O$) and iron (1M $C_6H_5FeO_7$) stocks were made in distilled water. Iron stock was made at least 3 days prior to use with occasional vortexing and mild heating to keep the ferric citrate in solution. In both cases, copper or iron stock was added after YPD was autoclaved, roughly 1 hr before the addition of yeast culture.

Each growth rate assay was initiated in a similar manner to the IC_{50} assays. Cultures from BY4741 and all CBM lines were struck from frozen and grown on YPD plates incubated at 30° for 2–3 days. Four or five colonies from BY4741 and a single colony from each CBM line was then inoculated into 10 ml YPD, shaking overnight at 30°. Optical density from overnight culture was standardized, and a 1:101 dilution was conducted into the appropriate medium. For each line, five random wells spanning two 100-well honeycomb plates were filled with 150 μl of diluted culture. Plates were incubated at 30° with maximum shaking for 24 hr in a Bioscreen C, with automated OD readings every 30 min. From the raw data, we extracted the maximum growth rate using a nonparametric spline fit performed by a custom R script (Gerstein *et al.* 2012). The maximum growth rates from the replicates of each CBM line were statistically compared against all replicates initiated from BY4741 using a *t*-test (replicates involving separate wells from a single Bioscreen C plate).

Copper tolerance of deletion lines

To assess whether intragenic mutations that arose within our CBM lines are phenotypically similar to knockout mutations, we measured copper tolerance (IC_{50}) of 21 gene deletion lines (Giaever *et al.* 2002), representing all of the available knockouts for the characterized genes that had mutated in our study (excluding the uncharacterized YPL247C and YDL176W). BY4741 is the progenitor of both the deletion collection and our ancestral strain background, allowing a direct comparison of the impact of deleting these genes. Tolerance (IC_{50}) was determined as above from OD measurements taken across an array of copper concentrations at 24 hr. Tolerance assays were conducted in the Bioscreen C and replicated twice, running simultaneously on two different machines.

Tetrad dissections to isolate single mutations

To separate the effects of single mutations from other mutations present in the evolved lines (including extra copies of *CUP1*), we crossed all of the CBM lines with BY4739, which has a common genotype yet opposite mating type and different auxotrophies than BY4741, the progenitor of our lines. We then attempted to sporulate the resulting diploid lines, focusing on a subset that contained each common mutation or aneuploidy and the fewest number of additional mutations (~1/3 of the lines). Detailed methods are provided in File S1.

We encountered substantial difficulties in obtaining tetrads from our strains; BY4741, a derivative of S288C, is known to be a poor sporulator (Deutschbauer and Davis 2005; Ben-Ari *et al.* 2006). In particular, despite many attempts, no tetrads were obtained for CBM16 (*PMA1* mutation plus chrII aneuploidy), CBM26 (*PMA1* mutation plus chrI, chrV, and chrVIII aneuploidy), CBM29 (*PMA1* mutation plus chrII aneuploidy), CBM47 (*VTC1* mutation), or CBM55 (no mutation identified other than extra copies of *CUP1*).

We were able to sporulare CBM2 (chrII aneuploidy), CBM14 (*MAM3* mutation), CBM25 (*MLP1* and *ENA5* mutations), and CBM34 (*VTC4* mutation). CBM25 was not initially chosen for tetrad dissection but was dissected as a contaminate of CBM22 (*VTC1* plus chrVIII and chrXVI aneuploidy), as detected by subsequent sequencing. CBM25 contaminating cells were likely positively selected during the sporulation procedure given that the aneuploid lines in our experiment, like CBM22, had very low sporulation rates.

The genotype of resulting spores was then determined (see File S1; PCR primer information in Table 2). In brief, for CBM14 and CBM34 tetrad lines, *MAM3* and *VTC4*, respectively, were amplified by PCR. All SNPs showed the expected 2:2 segregation pattern in the four spores of each dissected tetrad. CBM25 spores were sequenced on Illumina HiSeq 2000, which is when the strain was discovered to be CBM25 (bearing a mutation in *MLP1* and *ENA5*), not CBM22. The segregation pattern for the additional copy of chrII in CBM2 spores was determined by the segregation patterns of *LYS2* alleles. To quantify the segregation patterns of *CUP1* among the spores, Southern blots with *CUP1*-specific probes were performed. We isolated genomic DNA and ran a Southern blot on three separate occasions for each spore. Band intensity was quantified in ImageJ (Abramoff *et al.* 2004) using the "background corrected density" macro to estimate *CUP1* copy number.

Fitness effect of single mutations on growth rate and copper tolerance

To measure the fitness effects of the mutations isolated by tetrad dissection, growth rate assays were conducted within the Bioscreen C using either YPD + 9 mM $CuSO_4$ ("copper9") or YPD, as described above with the following exceptions. Yeast was occasionally taken from a lawn plated from frozen cells rather than from single colonies (the sporulated lines had been bottlenecked to a single colony just prior to freezing, and so a second bottleneck at this stage was less essential). Optical density was not standardized for the copper9 experiments as this was deemed to have little effect on inferred growth rates. For each line, two (copper9) or four (YPD) nonadjacent wells were filled with 150 μl of diluted culture and allowed to grow for 24 hr. This procedure was performed three times in the copper9 environment, and once in YPD to determine whether these lines were affected in their ability to grow in the nutrient-rich environment. The mean maximum growth rate was determined for each Bioscreen C assay in the copper9 environment, and statistics were performed using these means as data points.

Copper tolerance was determined for a subset of spores through dose–response experiments as described for the knockout lines except that two separate Bioscreen C runs were performed, with two replicate wells per run (Figure S1). Specifically, we assayed IC_{50} for two spores (among all of the tetrads for each line) that carried mutations of interest but had low *CUP1* copy number.

Results

We recovered a broad spectrum of genetic changes across 34 lines exposed to initially inhibitory levels of copper (Figure 1, Table 1). Most lines contained multiple mutations, in contrast to our previous results in nystatin (Gerstein *et al.* 2012), which is consistent with the longer waiting period before growth observed (4–7 days with nystatin, 7–14 days with copper). All lines except for two (CBM2, one of the five lines isolated on the first day, and CBM55, one of the 11 lines isolated on the last day) contained one or more single base-pair mutations. In total, there were 57 unique base-pair changes, including four single base-pair deletions and one single base-pair insertion (the latter also resulted in an adjacent base-pair change). Beyond changes to single sites, there were several large-scale mutations. Twelve lines exhibited chromosomal aneuploidy (Figure 1B), and three lines (CBM6, CBM7, and CBM17) appeared to have low mtDNA coverage, outside of the range of lines from our previous study with nystatin (Figure 1C). In addition, two changes involved deletions within repetitive regions, one in

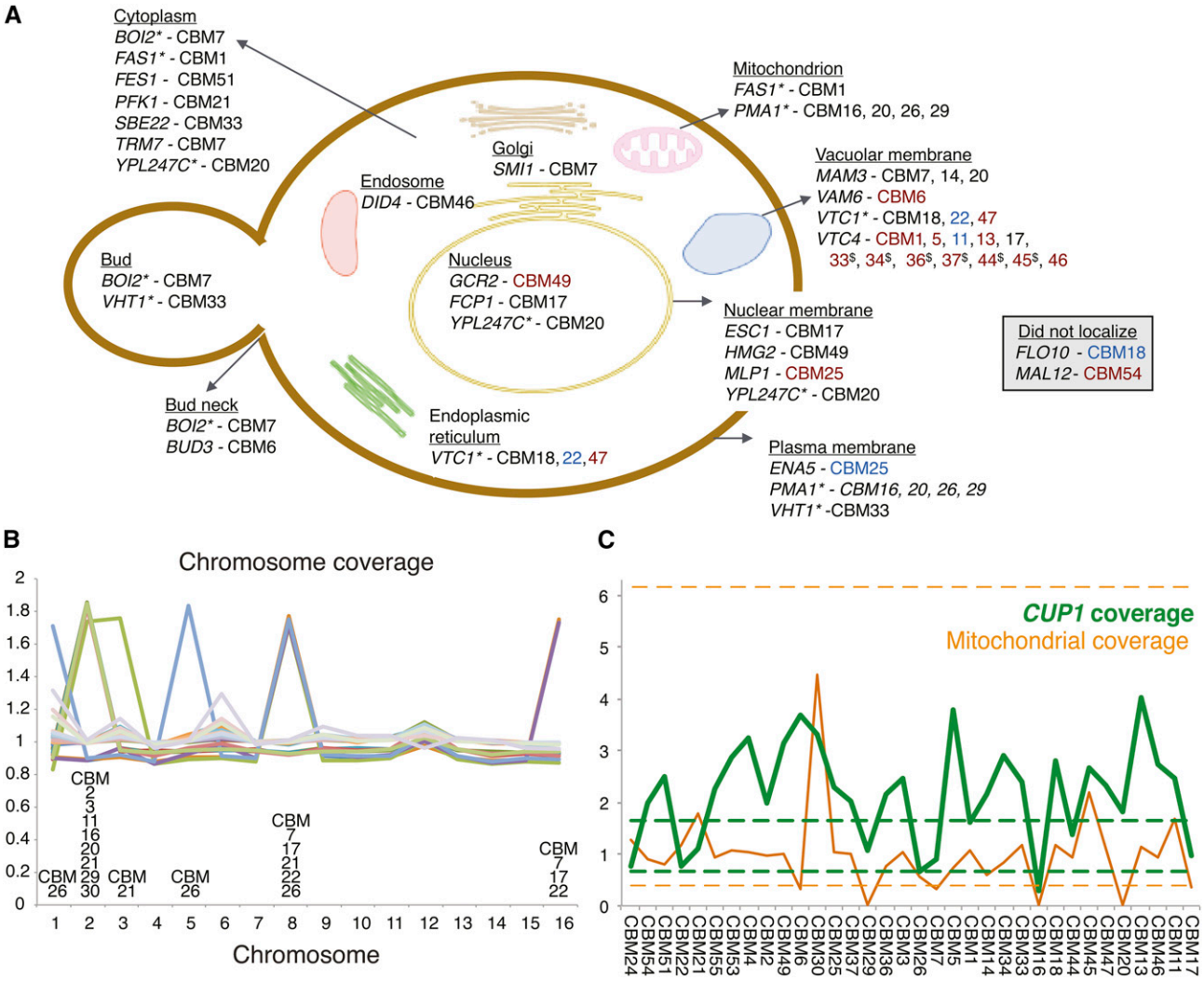

Figure 1 Observed mutations in copper-adaptation lines. (A) Genes mutated within the CBM lines (see Table 1 for specific mutations) illustrated based on previous localization studies of the genes involved (based on cellular component information curated at the Yeast Resource Center, http://www.yeastrc.org). The color of line names reflects the type of mutation: black for a nonsynonymous amino acid change, red for a premature stop codon, and blue for an indel or rearrangement (synonymous changes and RNA genes not shown). Genes that localized to more than one location are listed multiply and identified by "*." CBM lines 33, 34, 36, 37, and 45 contained the same *VTC4* mutation, indicated by "$." (B) Chromosomal coverage. Aneuploidy was prevalent, appearing in 12 of 34 lines. Coverage is determined by the average number of reads across the chromosome, compared to the reference strain. (C) *CUP1* copy number (green line) and mitochondrial coverage (orange line) for each CBM line. *CUP1* copy number is measured relative to the average level observed in our parallel nystatin study, which showed negligible variation in copy number (range of the 35 BMN lines shown as dashed green lines). Mitochondrial depth of coverage in the CBM lines was divided by 10 and is presented relative to the average depth of coverage from mapped nuclear DNA (the equivalent range for the 35 BMN lines shown as dashed orange lines). Lines are ordered according to increasing copper tolerance (Figure 2).

CBM25 involving the tandem array of P-type ATPase sodium pumps (*ENA5*, *ENA2*, and *ENA1*) and the second in CBM18 involving the flocculation gene *FLO10* (see details in Table 1).

The most frequent mutation across all lines was copy number alteration of the *CUP1* locus. Based on *in silico* qPCR, *CUP1* estimates were, on average, 2.17 times higher than estimates from the 35 lines obtained in nystatin. *CUP1* copy number was estimated to be above the entire range of nystatin lines for 24 of the 34 CBM lines, while two lines (CBM16 and 26) both exhibited *CUP1* levels lower than the range of nystatin lines (Figure 1C). *CUP1* is a metallothionein protein that binds copper in *S. cerevisiae*. It is present as a tandem duplication on chrVIII in the S288C reference strain, and amplification of this locus is known to be a common mutation that confers increased resistance to copper (Fogel and Welch 1982; Fogel *et al.* 1983; Adamo *et al.* 2012). Disomy for chrVIII has also been shown to increase copper tolerance (Fogel and Welch 1982). Indeed, including cases with chrVIII aneuploidy, 27 of the 34 CBM lines have increased *CUP1* copy number above the range of BMN lines (one of the exceptions, CBM24, is the least copper tolerant of our CBM lines).

When expression level of *CUP1* was investigated by qPCR in a subset of lines and compared with the *in silico* qPCR estimates, it was found that the slope was positive and significant when forced through the point (1,1), which assumes that both axes are scaled to the ancestor (even though,

technically, the derived nystatin lines and not BY4741 were used as the control in the *in silico* qPCR assays; $P = 0.02$, Figure S2A). The slope was still positive, but not significant otherwise ($P = 0.27$).

Single base-pair changes

Of the 57 unique single base-pair changes (Table 1), 15 were present in intergenic regions (2 of which were indels), and one single base-pair deletion was present in the intron of *COX1*. The remaining 41 unique single base-pair mutations were found within 29 different genes, whose products localize to many different cellular structures (Figure 1A). Five of these mutations were synonymous changes, 24 were nonsynonymous changes, 10 were premature stop codons, and 2 were frameshift mutations caused by single base-pair deletions.

Four sites were altered in the exact same way in multiple lines (a mutation at the intergenic site X.654261 in three lines, mito.24277 within an intron of *COX1* in seven lines, VII.480463 causing an amino acid change in *PMA1* in two lines, and X.412080 causing a stop codon in *VTC4* in six lines). As discussed previously (Gerstein *et al.* 2012), we cannot distinguish between repeated mutational hits and either a single ancestral mutation that amplified during the growth of the strain prior to being separated into lines (*i.e.*, during growth of the ancestral colony, followed by overnight growth in 10 ml YPD) or contamination during the sampling of lines on previous days. To be conservative, we consider the same mutation in multiple lines to be nonindependent and count them as having arisen only once in the statistical analyses below.

Four genes acquired multiple independent mutations, involving different positions in different strains. Fourteen lines acquired mutations in one of two subunits of the vacuolar transporter chaperone complex, *VTC1* (3 unique mutations in 3 lines) or *VTC4* (7 unique mutations in 12 lines); 4 lines acquired mutations in the plasma membrane H+-ATPase *PMA1* (3 unique mutations); and 3 lines acquired unique mutations in *MAM3*, a protein required for normal mitochondrial morphology (Entian *et al.* 1999).

Given the 6607 ORFs within the *S. cerevisiae* genome (http://www.yeastgenome.org/genomesnapshot), the data are enriched for multiply hit genes. Specifically, there is a 99% chance that the 41 genic mutations would either hit different genes (first line in equation 1) or would hit one gene twice but no more (second line in equation 1):

$$0.99 = \prod_{i=1}^{41} \frac{6607-(i-1)}{6607} + \sum_{j=2}^{41}\left(\prod_{i=1}^{j-1}\frac{6607-(i-1)}{6607}\right)\frac{j-1}{6607}\left(\prod_{i=j+1}^{41}\frac{6607-(i-2)}{6607}\right), \quad (1)$$

assuming that ORFs are roughly equal in length. Thus, seeing even one gene bearing mutations at three or more independent sites is highly unlikely, and we conclude that positive selection acted upon the mutations in *VTC1*, *VTC4*, *PMA1*, and *MAM3*.

Excluding the indels, the single base-pair mutations that occurred within exons generated a stop codon much more often than predicted by chance (10/39 = 25.6%, $P = 0.00006$, exact one-tailed binomial test with expectation of 5.78% based on the mutational spectrum in yeast, see *Materials and Methods*). This result remains marginally significant when we focus only on genes hit once and exclude the four multiply hit genes (4/25 = 16%, $P = 0.053$, expectation of 5.78%).

On the other hand, the fraction of unique mutations that fall within an exon rather than a noncoding region is not significantly greater than the expected fraction in *S. cerevisiae* (41/57 = 72.0%, $P = 0.63$, expectation of 72.9% from Alexander *et al.* 2010). Similarly, among the synonymous and nonsynonymous mutations, nonsynonymous changes did not occur more often than expected (including all changes: 24/29 = 82.8%, $P = 0.34$; excluding multiply hit genes: 16/21 = 76.2%, $P = 0.67$; both exact one-tailed binomial tests with an expected fraction of 77.6%). Furthermore, the mean exchangeability score (an empirically based measure of the change in protein function following a particular amino acid change; Yampolsky and Stoltzfus 2005) of our observed amino acid changes (0.294) was within one standard error of the grand mean for mutations in yeast (0.31, calculated based on the mutational spectrum reported in Lynch *et al.* 2008). These tests are likely conservative, however, because selection against deleterious amino acid changes would have eliminated nonsynonymous mutations from our dataset, making it difficult to detect an enrichment of amino acid changes due to positive selection.

The set of genes whose protein products were altered is not enriched for either a specific GO term or a particular pathway (based on YeastMine analysis; Balakrishnan *et al.* 2012), although a significant number of mutated genes localize to the plasma membrane (*PMA1*, *ENA5*, and *VHT1*), the nuclear membrane (*ESC1*, *HMG2*, *MLP1*, and *YPL247C*), and the vacuolar membrane (*MAM3*, *VAM6*, *VTC1*, and *VTC4*). The set of genes is also enriched for three of the MIPS functional classification groups: vacuole or lysosome (*VAM6*, *VTC1*, and *VTC4*), cation transport (*ENA5*, *PMA1*, and *VTC1*), and protein synthesis (*TRM7* and *FES1*) (identified using Funspec; Robinson *et al.* 2002).

Of the characterized genes that bore mutations, 21 were available from the yeast knockout collection (Giaever *et al.* 2002). Relative to BY4741, 13 lines showed a significant increase in copper tolerance, and two showed a significant decrease in copper tolerance (Figure S3). This assay supports the idea that a number of the singly hit genes might contain mutations that influenced copper tolerance.

To identify potential regulatory changes caused by the 15 intergenic mutations we found, we assessed whether predicted TF binding sites were gained or lost using Cis-BP (Weirauch *et al.* 2014) (Table S3). One of the positions (in *CBM1*) is not predicted to be at a TF binding site, while the remaining 14 were split among changes that caused both

gains and losses (five mutations), only gains (four mutations), and only losses (five mutations). We identified a number of commonalities among the mutations, including two sets of TF binding sites that were each lost together three times (one set involved members of the Forkhead family, *FKH2* and *HCM1*; and a second set involved *NHP6A*, *NHP6B*, and *PHO2*), two that were gained together three times (*GAT1* and *GLN3*, members of the GATA family), and some that were both gained and lost (particularly *ORC2* and *SUM1*). Among TF binding site mutations that were within 500 bp and 5′ of the start site of a gene, only one gene (*RPP1A*) was listed in the SGD as having an effect on metal tolerance, although two others affected vacuolar functioning (*MUK1* and YIR007W) and one affected mitochondrial functioning (*COX4*). We did not, however, directly measure the effects of the intergenic mutations.

Aneuploidies

Chromosomal aneuploidy was common, appearing in one-third of all CBM lines (Figure 1B). All aneuploid lines had an extra copy of either chrII or chrVIII (one line had both). chrII aneuploidy was generally found by itself, only one of the eight lines with chrII aneuploidy carried additional aneuploid chromosomes (chrIII and chrVIII). In contrast, chrVIII aneuploidy never appeared in isolation. Three of the five cases of chrVIII aneuploidy also contained an extra copy of chrXVI and one line contained additional copies of chrI and chrV (in addition to the aforementioned line containing chrII and chrIII).

Mutagenic effects of copper

While selection must underlie the repeated spread of mutations affecting the genes that were multiply hit, it is possible that copper exposure directly altered the rate and nature of mutations that arose during the experiment. Indeed, exposure to high concentrations of copper is known to be mutagenic in experiments that directly expose DNA to copper (Tkeshelashvili *et al.* 1991). There is no evidence, however, for an elevated base-pair mutation rate in our experiment. Focusing only on nucleotide changes (not indels), we observed 52 unique single base-pair changes across the 34 lines isolated over the course of 7–14 days (average 11.0 days until isolation; Table S1). By comparison, in our previous study where the same ancestral strain was exposed to nystatin, we observed 35 mutations among 35 lines isolated over the course of 4–7 days (average 4.7 days until isolation). Thus, if anything, slightly more mutations accumulated per line per day in nystatin (0.21) than in copper (0.14), although the difference is not significant ($P = 0.076$, two-tailed exact binomial test with $n = 52 + 35$ mutation events and a proportion expected in copper given by 0.693 given that there were 34 lines $\times$ 11.0 days in copper and 35 $\times$ 4.7 in nystatin). Furthermore, while previous *in vitro* work indicates that copper should induce an excess of G:C $\rightarrow$ A:T mutations (Tkeshelashvili *et al.* 1991), the spectrum of single base-pair mutations observed within this study (8 A:T $\rightarrow$ G:C, 14 G:C $\rightarrow$ A:T, 6 A:T $\rightarrow$ T:A, 12 G:C $\rightarrow$ T:A, 5 A:T $\rightarrow$ C:G, 7 G:C $\rightarrow$ C:G) is not significantly different from the mutational spectra for yeast reported by Lynch *et al.* (2008) (see their Table 1), either based on prior studies ($\chi^2 = 6.76$, d.f. = 5, $P = 0.239$) or based on their mutation-accumulation experiment ($\chi^2 = 1.48$, d.f. = 5, $P = 0.915$).

We did, however, observe many more aneuploid events with copper (affecting 12/34 lines) than with nystatin (affecting 1/35 lines; Gerstein *et al.* 2012), but this is only marginally significant if we account for the greater number of days until isolation ($P = 0.11$, two-tailed exact binomial test with $n = 12 + 1$ aneuploid lines, where the proportion expected in copper is 0.693). Here, we have treated multiple aneuploid chromosomes within a line as a single event, in the absence of information about their independence; if they were independent, the excess of aneuploid events in the presence of copper would be very significant ($P = 0.013$, two-tailed exact binomial test with $n = 19 + 1$ aneuploid chromosomes). An enrichment of aneuploid events in copper may well be due to selection for aneuploidy rather than an increased mutation rate, consistent with the frequent occurrence of additional copies of chrVIII, bearing *CUP1*. Nevertheless, previous studies with mice have found copper to be mutagenic, using a micronuclei assay that is sensitive to errors in chromosome segregation during mitosis (Prá *et al.* 2008). We thus consider it plausible that the high frequency of aneuploidy observed in this study may have been directly due to copper exposure.

Phenotypic assays of CBM lines

Copper tolerance (measured as IC_{50} in deep-well boxes grown for 72 hr) was fairly similar across the 34 copper-adapted CBM lines, ranging from 8.5 mM to 11.2 mM (Figure 2A). The date that mutations were isolated does not correlate with copper tolerance (mutations are numbered based on the date of isolation; Table S1). The number of copies of *CUP1* inferred from *in silico* qPCR (Figure 1C, corrected to include chrVIII aneuploidy) does not directly correlate with copper tolerance (Figure 2B; $r = 0.16$, $t_{32} = 0.92$, $P = 0.36$), yet this is likely due to the confounding effects of the other genetic changes. For example, three of the lines with the lowest *CUP1* copy number carried mutations in *PMA1* (excluding CBM24, which had low tolerance; Figure 2B). To tease apart the effects of these mutations, we both statistically analyzed the tolerance data collected for all lines and physically dissected the mutations via tetrad analysis in a subsample of four CBM lines (see below). A linear model with the four multiply hit genes as well as *CUP1* copy number and chrII aneuploidy as factors indicated that *CUP1* copy number (adjusted to include chrVIII aneuploidy) as well as the presence of a mutation in *MAM3*, *PMA1*, *VTC1*, or *VTC4* were all significant predictors of copper tolerance, while chrII aneuploidy was not (*CUP1* coverage: $t_{27} = 2.58$, $P = 0.016$; *VTC1*: $t_{27} = 3.73$, $P = 0.0009$; *PMA1*: $t_{27} = 2.99$, $P = 0.0060$; *MAM3*: $t_{27} = 3.11$, $P = 0.0044$; *VTC4*: $t_{27} = 6.66$, $P < 0.001$; and *chrII*: $t_{27} = 1.67$, $P = 0.11$).

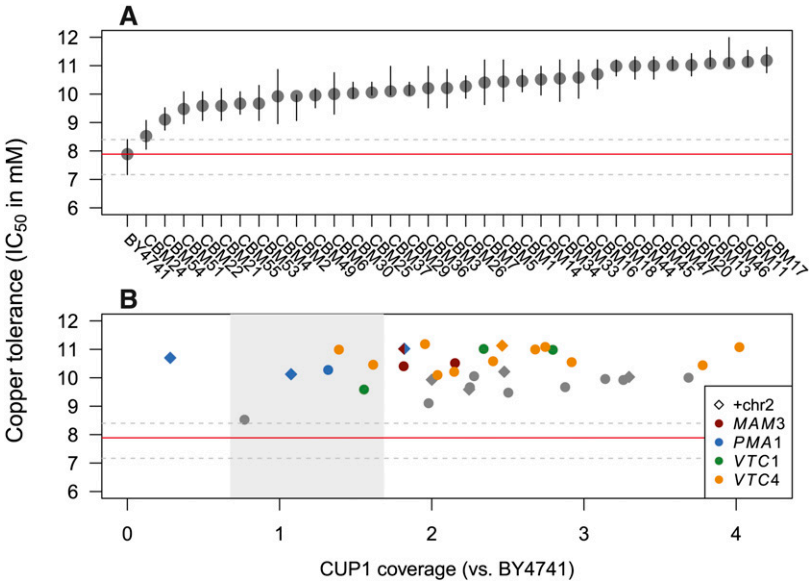

Figure 2 Copper tolerance across 34 copper-adapted lines ("CBM lines"). (A) Lines are numbered based on the date the mutant line was isolated following exposure to copper. The order of CBM lines in other graphs is based on the order of copper tolerance depicted here, which gives the IC_{50} after 72 hr of growth in deep-well boxes (bars represent 95% confidence intervals). Tolerance of BY4741 (the ancestor) is indicated by the horizontal red line with its confidence interval indicated by dashed gray lines. (B) Copper tolerance of each CBM line is generally high, regardless of the *CUP1* copy number (*x*-axis, accounting for duplication of chrVIII). The absence of a correlation between *CUP1* level and copper tolerance is due to the existence of additional mutations in the CBM lines, particularly in the four genes that were mutated independently (colors). Gray shading shows the range of *CUP1* observed among the BMN lines (see *Materials and Methods* and Figure 1C).

In addition to copper tolerance, we assayed maximum growth rates in copper, as well as YPD, YPG, and iron, using the Bioscreen C plate reader (Figure 3). Copper tended to be more inhibitory in the small volume plates used in the Bioscreen C, so we reduced copper levels to 8 mM $CuSO_4$ (copper8). Growth rate in copper8 (Figure 3A) was significantly correlated with copper tolerance (Figure 2A, $r = 0.69$, $t_{32} = 5.40$, $P < 0.0001$). All lines except CBM24 grew significantly faster in copper8 than did BY4741, the ancestor ($P < 0.05$, Table S4). Copper tolerance did not correlate with growth in any of the three other environments examined (Figure 3, B–D; YPD: $r = -0.31$, $t_{32} = -1.83$, $P = 0.077$; YPG: $r = -0.06$, $t_{32} = -0.34$, $P = 0.73$; and iron: $r = -0.09$, $t_{31} = -0.52$, $P = 0.61$). No lines exhibited significantly increased growth in the rich medium, YPD, while about half had significantly decreased growth (Table S5). There was a negative, but not significant correlation between growth in YPD and growth in copper or copper tolerance (IC_{50}). Three of the four slowest growing lines in YPD carried multiple aneuploid chromosomes (CBM17, 22, 26), but otherwise the slow growing lines spanned a range of genotypes and *CUP1* copy numbers. There was greater variation in growth rates observed in YPG and in iron, with growth in these two environments being strongly correlated ($r = 0.58$, $t_{31} = 3.98$, $P = 0.0004$; YPG statistical results in Table S6, iron results in Table S2). The 15 CBM lines that grew significantly slower in YPG and iron included all lines with *PMA1* mutations (CBM16, 20, 26, and 29), chrXVI aneuploidy (CBM7, 17, and 22), and chrII aneuploidy (CBM2, 3, 11, 16, 20, 21, 29, and 30), as well as all lines that lacked mtDNA (CBM16, 20, and 29).

Tetrad dissections to isolate single mutations

To examine the specific effect of common mutations, we crossed CBM2 (chrII aneuploidy), CBM14 (*MAM3*), CBM25 (*MLP1* and *ENA5*), and CBM34 (*VTC34*) to BY4739 and dissected the resulting tetrads. As indicated above each panel in Figure 4, the four mutations and chrII aneuploidy segregated according to a 2:2 pattern (±), but segregation of *CUP1* copy number was more variable (shown by colored circles). The variability in *CUP1* inheritance may reflect noise in the assay (band densities on Southern blots, even though measured in triplicate; Figure S2B), or it may indicate changes in *CUP1* over the course of the tetrad line construction. Indeed, previous work has shown copy number alterations were frequent (20%) during meiosis in lines heterozygous for *CUP1* (Welch *et al.* 1991).

Maximum growth rate in copper9 exhibited considerable variation among different spores from the same tetrad and rarely followed the strict 2:2 pattern expected if a single mutation underlay copper tolerance (Figure 4). The effect of each mutation on growth in copper is more easily seen in Figure 5, which shows linear fits through all of the tetrad data for a given CBM line (using the mean maximum growth rate across all replicates as a single data point for each spore). The interaction terms (seen as a difference in slope) were not significant, except for a marginally significant interaction between *VTC4* and *CUP1* ($t_{20} = 2.044$, $P = 0.054$, Figure 5D), and thus interactions were excluded from the main statistical analyses. For CBM14 and CBM34, the presence of a mutation in *MAM3* and *VTC4* (respectively), as well as *CUP1* copy number, had significant positive effects on growth rate (CBM14, *CUP1*: $t_{21} = 6.16$, $P < 0.0001$, *MAM3*: $t_{21} = 2.27$, $P = 0.034$; and CBM34, *CUP1*: $t_{21} = 6.16$, $P < 0.0001$, *VTC4*: $t_{21} = 4.41$, $P = 0.0002$). By contrast, only *CUP1* copy number had a significant effect on growth rate for CBM2 and CBM25 (CBM2, *CUP1*: $t_{13} = 2.66$, $P = 0.020$, +chrII: $t_{13} = 1.73$, $P = 0.11$; and CBM25, *CUP1*: $t_{12} = 3.37$, $P = 0.0056$, *MLP1*: $t_{12} = -0.30$, $P = 0.77$, *ENA5*: $t_{12} = -0.018$, $P = 0.99$).

The growth rate in copper9 may reflect an overall growth impact caused by the mutations, rather than a specific effect on growth in copper *per se*, interfering with our ability to detect improvement. To assess this possibility, we measured

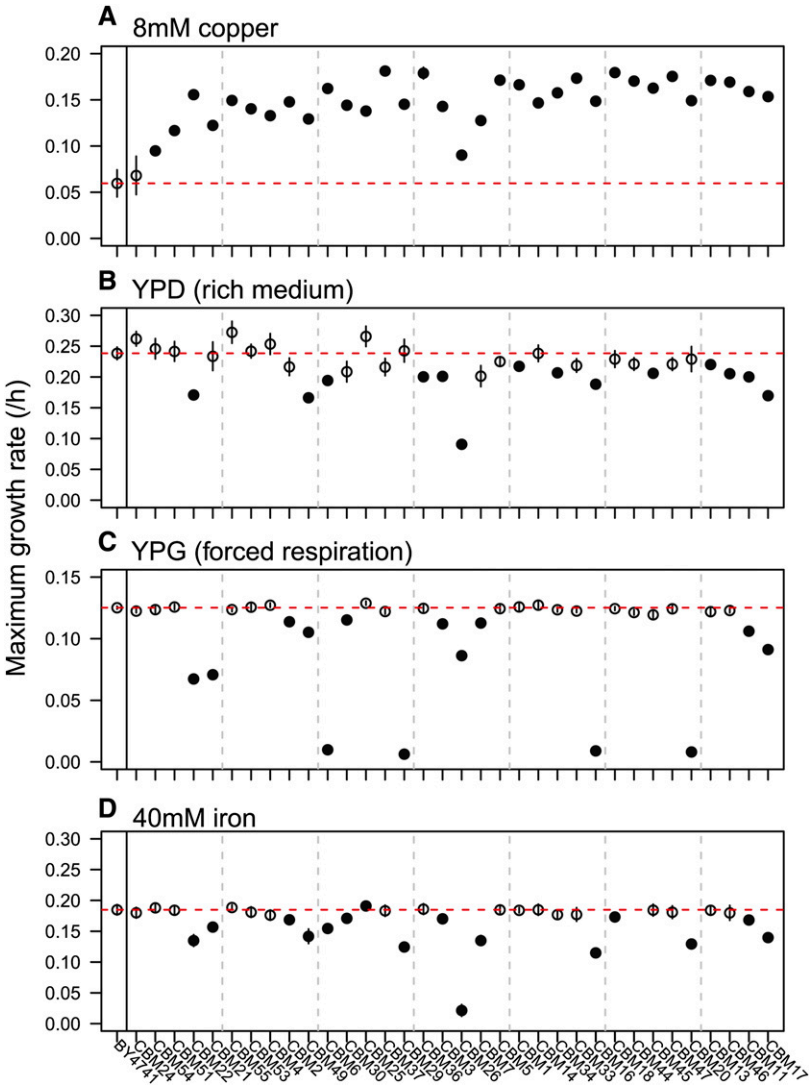

Figure 3 CBM lines have variable growth rates under different environmental conditions. Maximum growth rate (±1 SE) was assayed within the Bioscreen C in four different environments, each on a single day: (A) YPD + 8 mM $CuSO_4$, (B) YPD, a standard laboratory rich medium, (C) YPG, a medium that forces respiration, and (D) YPD + 40 mM ferric citrate. Closed circles are lines that are significantly different from the wild type, BY4741 (red dashed line; see Table S2, Table S4, Table S5, and Table S6 for statistical information). Vertical gray dashed lines are for ease of comparison among the panels.

growth in the rich medium, YPD, and reran the models performed above, using growth rate in YPD as the response variable. The models for CBM14, CBM25, and CBM34 contained no significant terms (Table S7). However, the model for CBM2 indicated that the presence of an extra copy of chrII contributed to a significant decrease in growth rate in YPD (Table S7, Figure S4). We thus reran the copper9 linear growth models for CBM2, adjusting for growth rate in YPD by taking the difference. This model indicated that chrII aneuploidy indeed has a significant positive effect on growth in copper when controlling for its negative effect on growth in YPD (Table S8).

Together, these tetrad analyses indicate that *CUP1* has a significant impact on growth in copper, as do the mutations in *MAM3* and *VTC4*. In addition, chrII aneuploidy has a significantly more positive impact on growth in copper than expected based on its negative effect on growth in YPD.

Finally, from among all tetrads available for each line, we measured copper tolerance (IC_{50}) for two spores that carried the mutation of interest (chrII aneuploidy, *MAM3*, *MLP1*, and *VTC4*) yet exhibited low *CUP1* copy number (Figure S1). All mutants were found to have a significantly higher copper tolerance than either the BY4741 ancestor or BY4739 parent (Figure S5), despite their low *CUP1* copy number. IC_{50} is likely to be a more sensitive assay of resistance to copper than maximum growth rate in a single copper level, suggesting that all of these mutations increase copper tolerance.

Reexamining the petite mutations

After the above analyses were conducted, we reexamined the lines that displayed small colonies on YPD plates (Table S1). To confirm that they were incapable of respiration, we assayed their growth on YPG plates. While 11 lines showed no growth, three lines (CBM9, 27, and 28) formed colonies, indicating that their mitochondria were still functional. These three lines were then whole-genome sequenced using population samples (Table S9). Line CBM9 carried a high-frequency SNP in *PMA1*, CBM27 carried a 3-bp deletion in *PMA1*, and CBM28 was aneuploid for chrIII, chrV, and chrVIII (a

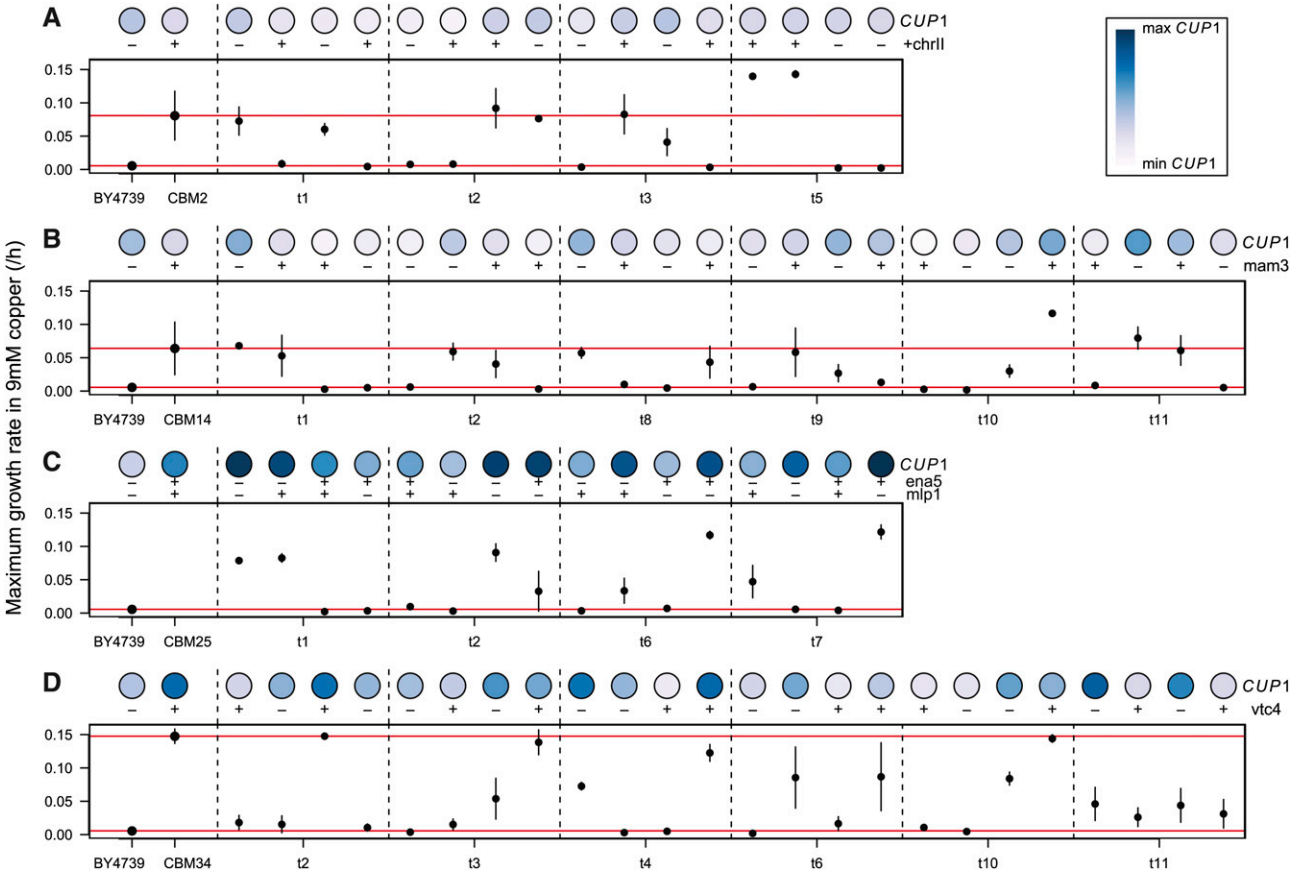

Figure 4 Maximum growth rates of tetrad lines in YPD + 9 mM $CuSO_4$. Tetrads were derived from four different CBM lines: (A) CBM2, (B) CBM14, (C) CBM25, and (D) CBM34. For each line, maximum growth rate was assayed within the Bioscreen C, with bars representing ±1 SE across 3 days. The darkness of the circle represents the line's relative number of copies of *CUP1*, as assayed by Southern blot. Presence (+) or absence (−) of a segregating mutation is also noted. The maximum growth rate is shown for all tetrad lines, as well as for their two parents, BY4739 and the relevant CBM parent (red lines), except for the tetrads derived from CBM25 for which parental growth rate was not assayed (due to its initially being considered CBM22, see *Materials and Methods*).

combination not seen in any other line). Levels of *CUP1* were assayed as in Figure 1C and fell within the range of the BMN lines (CBM9, 0.69; CBM27, 0.83; and CBM28, 1.25), except for CBM28 once we account for its extra copy of chrVIII. Altogether, these lines provide additional confirmation of the role of *PMA1* and chrVIII aneuploidy in the evolution of copper tolerance, although we infer that the mutational routes taken by these three lines were particularly deleterious in the absence of copper, given their small colony size on YPD plates.

Discussion

Depending on the different possible directions in which the environment may change, how rapidly can evolution happen and via how many different possible pathways? The advent of rapid sequencing technology has led to an increase in studies examining the repeatability of evolution at the level of the genotype, finding that the same genes often underlie parallel and convergent evolution in natural populations and during experimental evolution studies (Conte *et al.* 2012; Martin and Orgogozo 2013, see references within). Whether this repeatability reflects convergence over time to fitter genotypes or a limited scope of adaptive mutations along the way remains unknown. Also unknown is the relationship between the type of evolutionary challenge and the likelihood of parallel genetic changes (Stern 2013). This study aimed to contribute to our understanding of how the type of environmental challenge influences the genomic target size of the mutations selected during the very first steps of adaptation. We used the same mutation acquisition protocol as in our previous study on nystatin resistance (Gerstein *et al.* 2012) to obtain mutations in the presence of an inhibitory level of copper. We predicted that a broader range of genetic solutions would underlie copper adaptation, in contrast to the nystatin study that identified a narrow genetic solution (all 35 lines had mutations within four genes in the same pathway). Previous studies have suggested that xenobiotic environments (such as antimicrobial drugs) select for repeated genetic solutions (Martin and Orgogozo 2013). By contrast, copper is a very different kind of environmental stressor—it is essential for several different enzymatic processes in yeast (Graden and Winge 1997) and therefore cannot be blocked entirely from entering the cell. Copper is,

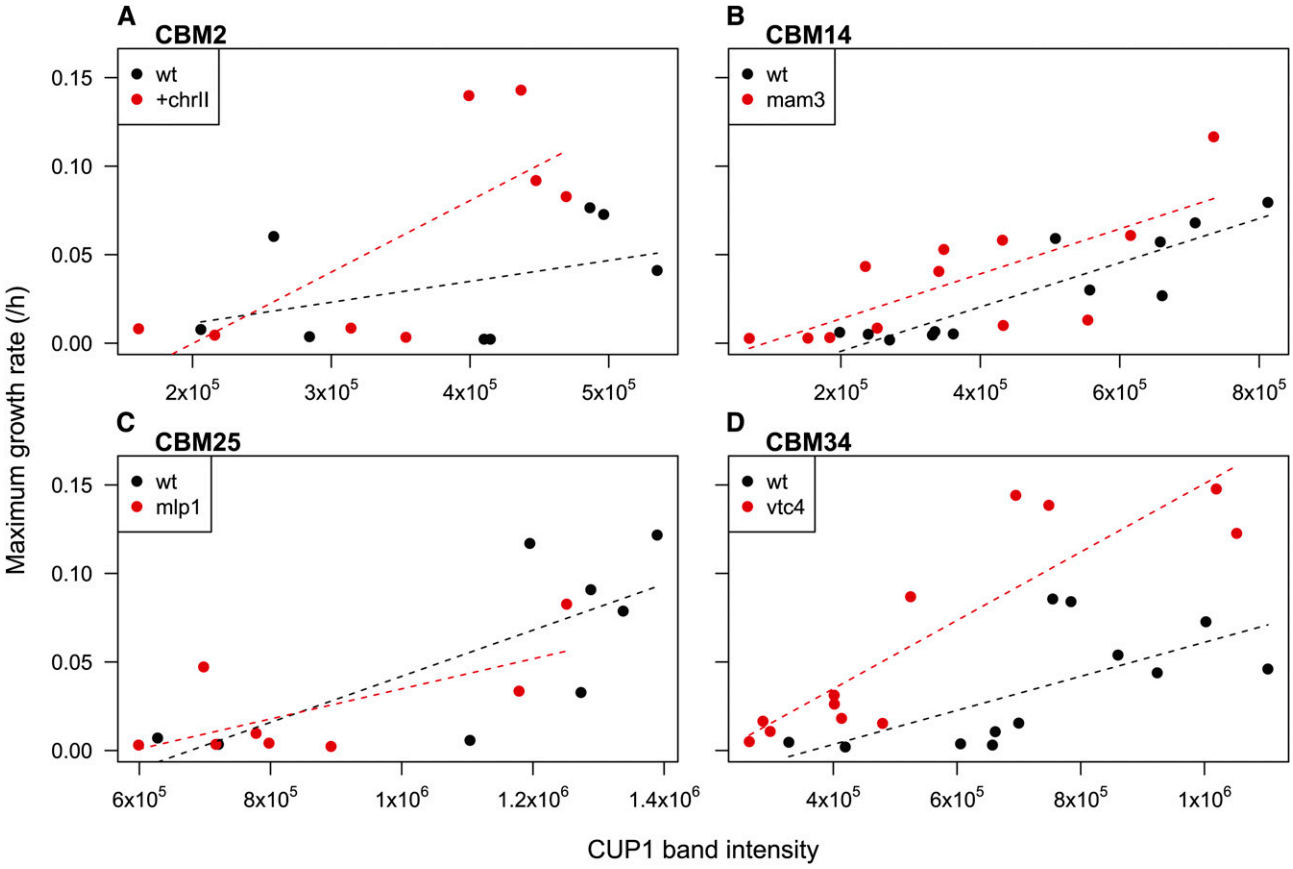

Figure 5 Impact of mutations on growth of tetrad lines in YPD + 9 mM $CuSO_4$. Dots indicate maximum growth rates for tetrad lines carrying (red) or lacking (black) the mutation of interest: (A) chrII aneuploidy in CBM2, (B) *MAM3* in CBM14, (C) *MLP1* in CBM25, and (D) *VTC4* in CBM34. For each line, linear model fits were performed with maximum growth rate as the response variable and *CUP1* copy number and the allele status of the other mutation as the predictors. All fits are plotted including interaction terms between *CUP1* copy number and the other gene of interest, where *MLP1* was used as the gene of interest for CBM25 in C (no difference is seen when using *ENA5*).

however, toxic at high concentrations (Peña *et al.* 1999), and thus its concentration in the cell must be held in a delicate balance. As predicted, we identified a large number of mutations among our copper adaptation lines, with the level of genetic parallelism highly dependent on the type of mutation under investigation.

Increased copy number of the *CUP1* locus through tandem duplication or aneuploidy of chrVIII was by far the most common mutation, seen in 27 of the 34 copper adaptation lines. *CUP1* exists as a tandem repeat in the S288C genome, and adaptation under copper stress has previously been shown to select for amplification of this locus (Fogel and Welch 1982; Adamo *et al.* 2012). Indeed, Covo *et al.* (2014) recently demonstrated that moving *CUP1* onto other chromosomes can efficiently select for disomy under copper stress. The number of *CUP1* copies varies among naturally isolated wild and vineyard strains (between 1 and 18 copies among 14 wild strains, Zhao *et al.* 2014, and 4 and 18 copies among 15 Italian vineyard strains, Stroobants *et al.* 2008). As *CUP1* is present in the ancestral genome as a tandem repeat, it is likely prone to alterations in copy number as a consequence of unequal crossover, gene conversion, or single-strand annealing (Zhang *et al.* 2013). Furthermore, *CUP1* amplification seems to incur few pleiotropic costs, as seen by the lack of an observed effect of *CUP1* copy number on growth rate in YPD among our tetrad lines (Table S7).

Chromosomal aneuploidy also repeatedly arose within our lines. Twelve of the 34 lines were aneuploid, and each of these 12 lines contained either chrVIII aneuploidy (5 lines) or chrII aneuploidy (8 lines). Chromosomal aneuploidy seems to be a common route to adaptation for fungal species reproducing asexually in a diverse array of environmental stressors such as drug resistance (Selmecki *et al.* 2009; Sionov *et al.* 2010), high temperature (Yona *et al.* 2012), and salt (Dhar *et al.* 2011). Aneuploidy is an intriguing beneficial mutation, as it has the potential to affect many genes simultaneously, yet has a much higher reversion rate than other types of mutations. Whether such a high degree of aneuploidy would have been seen had our strains evolved for longer remains an open question. It may be that aneuploidy serves primarily as a stop-gap adaptation until other beneficial mutations appear in the genome with fewer costs (Yona *et al.* 2012). In our experiment, chrVIII aneuploidy may have been positively selected for its effect on *CUP1* copy number, as seen by Fogel and Welch (1982). Similarly, chrII aneuploidy had a more beneficial effect in copper (Figure 5, Table S8) than

expected, based on its low growth in YPD (Table S7), perhaps because it amplified genes contributing to copper tolerance, such as *SCO1* and *SCO2* (nonadjacent gene duplicates on chrII), which function in the delivery of copper to cytochrome c oxidase in the mitochondrial inner membrane. ChrII aneuploidy was also repeatedly observed by Covo *et al.* (2014) when investigating chromosomes gained in response to copper stress. Whether the other aneuploid chromosomes had an effect on copper tolerance remains unknown. Repeated attempts to sporulate CBM22 (aneuploid for chrVIII and chrXVI) and CBM26 (aneuploid for chrI, chrV, and chrVIII) failed to yield tetrads.

The major genetic contributors to copper tolerance besides *CUP1* were four genes involved in maintaining plasma membrane potential (*PMA1*), vacuolar transport (*VTC1* and *VTC4*), and mitochondrial morphology (*MAM3*). These genes each bore several independent protein-coding mutations in different lines, which is highly unlikely in the absence of selection. Indeed, of the seven lines that did not exhibit *CUP1* amplification (relative to the range of BMN lines), six involved mutations in these genes (three in *PMA1*, one in *VTC1*, and two in *VTC4*), with the remaining low-*CUP1* line exhibiting little copper tolerance (CBM24).

The types of mutations observed in *VTC4* and *VTC1* point to selection for loss of function in these genes, with several mutations inducing stop codons or frame shifts (Table 1). Furthermore, deletion of *VTC1* and *VTC4*, as well as *MAM3*, significantly increased copper tolerance (Figure S3). By contrast, *PMA1* codes for a plasma membrane H+-ATPase that regulates cytoplasmic pH, and yeast are inviable when this gene is deleted. High levels of copper have previously been shown to have a deleterious effect on plasma membrane organization (Fernandes *et al.* 2000), while strongly stimulating plasma membrane ATPase activity (Fernandes and Sá-Correia 2001). It thus seems likely that the mutations identified in *PMA1* alter, rather than inactivate, this protein, suggesting a gain (or fine tuning) of function. Consistent with this view, none of the *PMA1* mutations involved stop codons or frameshifts (neither the four listed in Table 1 nor the two additional *PMA1* mutations among the lines initially categorized as petites, Table S9).

In addition, 25 genes bore a single mutation in a single line in our experiment (Table 1). These unique mutations were no more likely to be nonsynonymous than expected, based on the mutational spectrum and no more likely to occur within exons than expected. That said, several of the unique mutations caused stop codons (4/25), a marginally significant excess. Furthermore, 12/18 of the deletion lines tested for this subset of genes were found to have significantly altered copper tolerance when compared to BY4741 (Figure S3), suggesting that at least some of the uniquely hit genes may be playing a role in copper tolerance. Alternatively, many of the mutations in singly hit genes may have been neutral but spread via hitchhiking, a pervasive phenomenon in other batch culture experiments (Lang *et al.* 2013).

Beyond genetic changes, epigenetic changes may have contributed to copper adaptation. This possibility was not formally investigated in our study. We can, however, conclude that epigenetic change was not the primary cause of adaptation, given that plausible causative mutations, involving either *CUP1* or the four multiply hit genes, occurred in every line except one (Table 1, Figure 2B). The exception, CBM24, was the least copper tolerant line, bore only two intergenic mutations, and remains a possible candidate for epigenetic adaptation, although our genomic analysis may not have found all rearrangements or changes in hard-to-align regions.

One question of interest is why our copper-adapted lines carried so many more mutations, on average, than the nystatin-adapted lines studied previously (Gerstein *et al.* 2012). In no case did we see a BMN line that carried two mutations thought to be adaptive; all lines carried one and only one mutation in an *ERG* gene. By contrast, 21 of the 34 CBM lines carried more than one mutation for which we have evidence of a beneficial effect in copper (including the four multiply hit genes, chrII aneuploidy, and *CUP1* levels above the BMN range when including chrVIII aneuploidy; 15 of 34 lines if we exclude chrII aneuploidy). The greater contribution of multiple beneficial changes to copper adaptation cannot be explained by a larger pool of large-effect beneficial mutations or a higher mutation rate, because it took longer to observe growth in copper (7–14 days) than in nystatin (4–7 days). One possibility is that many of the adaptive mutations may not have been beneficial enough on their own to generate detectable growth; instead, they may have allowed a line to persist for longer or to expand slightly in population size, facilitating the appearance of subsequent large-effect mutations. An alternative possibility is that positive epistasis among mutations more strongly favored the spread of secondary mutations. Our tetrad analysis provides some evidence for this possibility. Figure 5 shows that the effect of *VTC4* on growth rate rises with *CUP1* copy number among tetrads of CBM34, a marginally significant positive interaction ($t_{20} = 2.044$, $P = 0.054$). Similarly, the benefits of chrII aneuploidy also appear mild at low *CUP1* levels and rise with increasing *CUP1* copy number among CBM2 tetrads, although this interaction is not significant ($t_{12} = 1.61$, $P = 0.13$). In accordance with either of these explanations (mutations facilitating subsequent adaptation or positive epistasis), *VTC4* mutations occurred more often among the CBM lines with higher *CUP1* copy numbers (Table 1, Figure 2B).

This study provides an in depth analysis of how a eukaryotic organism, like yeast, takes its first few evolutionary steps toward tolerating an inhibitory but essential element, copper. Our genome-wide analysis of 34 strains found that adaptation often involved a common step (especially amplification of *CUP1*), but that routes less taken were also available. These alternate routes often involved chromosomal aneuploidy of chrII or chrVIII and four genes with roles in a wide variety of cellular functions—vacuolar transporters, mitochondrial morphology, and cytoplasmic pH regulation.

Compared to our previous study of nystatin resistance (Gerstein *et al.* 2012), the variety of genes allowing growth in copper suggests that altered environments with more widespread effects on a cell may also provide a broader genetic basis for evolutionary recovery. Previous longer-term experimental evolution studies with microbes (*e.g.*, Conrad *et al.* 2009; Miller *et al.* 2011; Tenaillon *et al.* 2012; Wong *et al.* 2012; Herron and Doebeli 2013; Lang *et al.* 2013; Kryazhimskiy *et al.* 2014) have found a high degree of parallel evolution at the gene level, and our results suggest that this can be the case even among the very first mutations selected. Whether adaptive mutations are likely to recur depends, in theory, on the effect size of the mutations as well as their mutation rate. In our case, amplification of *CUP1* is both a relatively large effect mutation and easily acquired, contributing to its highly repeated nature, but it was also aided by the beneficial effects of many other less repeated mutations. In short, adaptation to copper is both more and less repeatable than adaptation to nystatin, with adaptation via *CUP1* representing the route most commonly taken, but with mutations affecting a variety of other cellular processes providing a diversity of less traveled paths toward copper adaptation.

Acknowledgments

We are grateful to Sherry Li, Anna Van Tol, William Li, Xinya Wang, and Angelica Lillico-Ouachour for assistance in the lab; Barry Williams for helpful discussions regarding the genes involved in copper adaptation; Chris Walkey for advice on sporulation; Krystina Ho for advice on tetrad dissection; Patricia Schulte and Tim Healy for assistance running and analyzing qPCR results; Vivien Measday and Corey Nislow for assistance with the deletion lines; Martin Kircher and Edward Fox for discussions regarding the mutagenic properties of copper; and to two reviewers for their helpful comments on the manuscript. This work was supported by the National Science and Engineering Research Council of Canada (A.C.G. and S.P.O.), the Killam Trusts (A.C.G.), and a University of British Columbia graduate fellowship to J.O.

Literature Cited

Abramoff, M., P. Magalhaes, and S. Ram, 2004 Image processing with ImageJ. Biophotonics International 11: 36–42.

Adamo, G. M., M. Lotti, M. J. Tamás, and S. Brocca, 2012 Amplification of the CUP1 gene is associated with evolution of copper tolerance in Saccharomyces Cerevisiae. Microbiol. 158: 2325–35.

Alexander, R. P., G. Fang, J. Rozowsky, M. Snyder, and M. B. Gerstein, 2010 Annotating non-coding regions of the genome. Nat. Rev. Genet. 11: 559–571.

Balakrishnan, R., J. Park, K. Karra, B. C. Hitz, G. Binkley *et al.*, 2012 YeastMine—an integrated data warehouse for *Saccharomyces cerevisiae* data as a multipurpose tool-kit. Database 2012: bar062.

Bell, G., and S. Collins, 2008 Adaptation, extinction and global change. Evol. Appl. 1: 3–16.

Ben-Ari, G., D. Zenvirth, A. Sherman, L. David, M. Klutstein *et al.*, 2006 Four linked genes participate in controlling sporulation efficiency in budding yeast. PLoS Genet. 2: e195.

Burch, C. L., and L. Chao, 1999 Evolution by small steps and rugged landscapes in the RNA virus phi6. Genetics 151: 921–927.

Chou, H. H., H. C. Chiu, N. F. Delaney, D. Segre, and C. J. Marx, 2011 Diminishing returns epistasis among beneficial mutations decelerates adaptation. Science 332: 1190–1192.

Conrad, T. M., A. R. Joyce, M. K. Applebee, C. L. Barrett, B. Xie *et al.*, 2009 Whole-genome resequencing of *Escherichia coli* K-12 MG1655 undergoing short-term laboratory evolution in lactate minimal media reveals flexible selection of adaptive mutations. Genome Biol. 10: R118.

Conte, G. L., M. E. Arnegard, C. L. Peichel, and D. Schluter, 2012 The probability of genetic parallelism and convergence in natural populations. Proc. Biol. Sci. 279: 5039–5047.

Covo, S., C. M. Puccia, J. L. Argueso, D. A. Gordenin, and M. A. Resnick, 2014 The sister chromatid cohesion pathway suppresses multiple chromosome gain and chromosome amplification. Genetics 196: 373–384.

Deutschbauer, A. M., and R. W. Davis, 2005 Quantitative trait loci mapped to single-nucleotide resolution in yeast. Nat. Genet. 37: 1333–1340.

Dhar, R., R. Sägesser, C. Weikert, J. Yuan, and A. Wagner, 2011 Adaptation of Saccharomyces cerevisiae to saline stress through laboratory evolution. J. Evol. Biol. 24: 1135–1153.

Entian, K.-D., T. Schuster, J. Hegemann, D. Becher, H. Feldmann *et al.*, 1999 Functional analysis of 150 deletion mutants in *Saccharomyces cerevisiae* by a systematic approach. Mol. Gen. Genet. 262: 683–702.

Fernandes, A. R., M. Prieto, and I. Sá-Correia, 2000 Modification of plasma membrane lipid order and H+-ATPase activity as part of the response of *Saccharomyces cerevisiae* to cultivation under mild and high copper stress. Arch. Microbiol. 173: 262–268.

Fernandes, A. R., and I. Sá-Correia, 2001 The activity of plasma membrane H(+)-ATPase is strongly stimulated during *Saccharomyces cerevisiae* adaptation to growth under high copper stress, accompanying intracellular acidification. Yeast 18: 511–521.

Fisher, R. A., 1930 *The Genetical Theory of Natural Selection*, Oxford University Press, Oxford.

Fogel, S., and J. W. Welch, 1982 Tandem gene amplification mediates copper resistance in yeast. Proc. Natl. Acad. Sci. USA 79: 5342–5346.

Fogel, S., J. W. Welch, G. Cathala, and M. Karin, 1983 Gene amplification in yeast: *CUP1* copy number regulates copper resistance. Curr. Genet. 7: 347–355.

Fogle, C. A., J. L. Nagle, and M. M. Desai, 2008 Clonal interference, multiple mutations and adaptation in large asexual populations. Genetics 180: 2163–2173.

Gerstein, A. C., D. S. Lo, and S. P. Otto, 2012 Parallel genetic changes and non-parallel gene-environment interactions underlie drug resistance in yeast. Genetics 192: 241–252.

Gerstein, A. C., A. Kuzmin, and S. P. Otto, 2014 Loss of heterozygosity facilitates passage through Haldane's sieve. Nat. Genet. 5: 3819.

Giaever, G., A. M. Chu, L. Ni, C. Connelly, L. Riles *et al.*, 2002 Functional profiling of the *Saccharomyces cerevisiae* genome. Nature 418: 387–391.

Gompel, N., and B. Prud'homme, 2009 The causes of repeated genetic evolution. Dev. Biol. 332: 36–47.

Gompel, N., B. Prud'homme, P. J. Wittkopp, V. A. Kassner, and S. B. Carroll, 2005 Chance caught on the wing: *cis*-regulatory evolution and the origin of pigment patterns in *Drosophila*. Nature 433: 481–487.

Gould, S., 1989 *Wonderful Life: The Burgess Shale and the Nature of History*, Norton, New York.

Graden, J. A., and D. R. Winge, 1997 Copper-mediated repression of the activation domain in the yeast Mac1p transcription factor. Proc. Natl. Acad. Sci. USA 94: 5550–5555.
Herron, M. D., and M. Doebeli, 2013 Parallel evolutionary dynamics of adaptive diversification in *escherichia coli*. PLoS Biol. 11: e1001490.
Huse, H. K., T. Kwon, J. E. A. Zlosnik, D. P. Speert, E. M. Marcotte *et al.*, 2010 Parallel evolution in *Pseudomonas aeruginosa* over 39,000 generations *in vivo*. MBio 1: e00199–e001910.
Kryazhimskiy, S., D. Rice, E. Jerison, and M. Desai, 2014 Global epistasis makes adaptation predictable despite sequence-level stochasticity. Science 344: 1519–1522.
Kvitek, D. J., and G. Sherlock, 2011 Reciprocal sign epistasis between frequently experimentally evolved adaptive mutations causes a rugged fitness landscape. PLoS Genet. 7: e1002056.
Lang, G. I., D. P. Rice, M. J. Hickman, E. Sodergren, G. M. Weinstock *et al.*, 2013 Pervasive genetic hitchhiking and clonal interference in forty evolving yeast populations. Nature 500: 571–574.
Li, H., B. Handsaker, A. Wysoker, T. Fennell, J. Ruan *et al.*, 2009 The sequence alignment/map format and SAMtools. Bioinformatics 25: 2078–2079.
Losos, J. B., 1992 The evolution of convergent structure in Caribbean *Anolis* communities. Syst. Biol. 41: 403–420.
Lynch, M., W. Sung, K. Morris, N. Coffey, and C. Landry, 2008 A genome-wide view of the spectrum of spontaneous mutations in yeast. Proc. Natl. Acad. Sci. USA 105: 9272–9277.
Manceau, M., V. S. Domingues, C. R. Linnen, E. B. Rosenblum, and H. E. Hoekstra, 2010 Convergence in pigmentation at multiple levels: mutations, genes and function. Philos. Trans. R. Soc. Lond. B Biol. Sci. 365: 2439–2450.
Martin, A., and V. Orgogozo, 2013 The loci of repeated evolution: a catalog of genetic hotspots of phenotypic variation. Evolution 67: 1235–1250.
Miller, C., P. Joyce, and H. Wichman, 2011 Mutational effects and population dynamics during viral adaptation challenge current models. Genetics 187: 185.
Peña, M., J. Lee, and D. Thiele, 1999 A delicate balance: homeostatic control of copper uptake and distribution. J. Nutr. 129: 1251–1260.
Prá, D., S. I. R. Franke, R. Giulian, M. L. Yoneama, J. F. Dias *et al.*, 2008 Genotoxicity and mutagenicity of iron and copper in mice. Biometals 21: 289–297.
Prud'homme, B., N. Gompel, A. Rokas, V. A. Kassner, T. M. Williams *et al.*, 2006 Repeated morphological evolution through *cis*-regulatory changes in a pleiotropic gene. Nature 440: 1050–1053.
Robinson, M. D., J. Grigull, N. Mohammad, and T. R. Hughes, 2002 FunSpec: a web-based cluster interpreter for yeast. BMC Bioinformatics 3: 35.
Rozen, D., J. de Visser, and P. Gerrish, 2002 Fitness effects of fixed beneficial mutations in microbial populations. Curr. Biol. 12: 1040–1045.
Sambrook, J., and D. W. Russell, 2001 *Molecular Cloning: A Laboratory Manual*, Ed. 3. Cold Spring Harbor Laboratory Press, Cold Spring Harbor, NY.
Schluter, D., E. A. Clifford, M. Nemethy, and J. S. McKinnon, 2004 Parallel evolution and inheritance of quantitative traits. Am. Nat. 163: 809–822.
Schneeberger, K., 2014 Using next-generation sequencing to isolate mutant genes from forward genetic screens. Nature Publishing Group 15: 662–676.
Selmecki, A. M., K. Dulmage, L. E. Cowen, J. B. Anderson, and J. Berman, 2009 Acquisition of aneuploidy provides increased fitness during the evolution of antifungal drug resistance. PLoS Genet. 5: e1000705.
Sionov, E., H. Lee, Y. C. Chang, and K. J. Kwon-Chung, 2010 *Cryptococcus neoformans* overcomes stress of azole drugs by formation of disomy in specific multiple chromosomes. PLoS Pathog. 6: e1000848.
Stern, D. L., 2000 Perspective: evolutionary developmental biology and the problem of variation. Evolution 54: 1079–1091.
Stern, D. L., 2013 The genetic causes of convergent evolution. Nat. Rev. Genet. 14: 751–764.
Stroobants, A., J.-M. Delroisse, F. Delvigne, J. Delva, D. Portetelle *et al.*, 2008 Isolation and biomass production of a *Saccharomyces cerevisiae* strain binding copper and zinc ions. Appl. Biochem. Biotechnol. 157: 85–97.
Tenaillon, O., A. Rodriguez-Verdugo, R. L. Gaut, P. McDonald, A. F. Bennett *et al.*, 2012 The molecular diversity of adaptive convergence. Science 335: 457–461.
Teste, M.-A., M. Duquenne, J. M. Francois, and J.-L. Parrou, 2009 Validation of reference genes for quantitative expression analysis by real-time RT-PCR in *Saccharomyces cerevisiae*. BMC Mol. Biol. 10: 99.
Tkeshelashvili, L., T. McBride, K. Spence, and L. Loeb, 1991 Mutation spectrum of copper-induced DNA damage. J. Biol. Chem. 266: 6401–6406.
Weirauch, M. T., A. Yang, M. Albu, A. G. Cote, A. Montenegro-Montero *et al.*, 2014 Determination and inference of eukaryotic transcription factor sequence specificity. Cell 158: 1431–1443.
Welch, J., D. Maloney, and S. Fogel, 1991 Gene conversions within the *Cup1*^{r} region from heterologous crosses in *Saccharomyces cerevisiae*. Mol. Gen. Genet. 229: 261–266.
Wenger, J. W., J. Piotrowski, S. Nagarajan, K. Chiotti, G. Sherlock *et al.*, 2011 Hunger artists: yeast adapted to carbon limitation show trade-offs under carbon sufficiency. PLoS Genet. 7: e1002202.
Wong, A., N. Rodrigue, and R. Kassen, 2012 Genomics of adaptation during experimental evolution of the opportunistic pathogen *pseudomonas aeruginosa*. PLoS Genet. 8: e1002928.
Woods, R., 1971 Nystatin-resistant mutants of yeast: alterations in sterol content. J. Bacteriol. 108: 69–73.
Yampolsky, L. Y., and A. Stoltzfus, 2005 The exchangeability of amino acids in proteins. Genetics 170: 1459–1472.
Yona, A. H., Y. S. Manor, R. H. Herbst, G. H. Romano, A. Mitchell *et al.*, 2012 Chromosomal duplication is a transient evolutionary solution to stress. Proc. Natl. Acad. Sci. USA 109: 21010–21015.
Zhang, H., A. F. B. Zeidler, W. Song, C. M. Puccia, E. Malc *et al.*, 2013 Gene copy-number variation in haploid and diploid strains of the yeast *Saccharomyces cerevisiae*. Genetics 193: 785–801.
Zhao, Y., P. K. Strope, S. G. Kozmin, J. H. McCusker, F. S. Dietrich *et al.*, 2014 Structures of naturally evolved *cup1* tandem arrays in yeast indicate that these arrays are generated by unequal non-homologous recombination. G3 4: 2259–2269.

Communicating editor: S. I. Wright

GENETICS

Supporting Information
http://www.genetics.org/lookup/suppl/doi:10.1534/genetics.114.171124/-/DC1

Too Much of a Good Thing: The Unique and Repeated Paths Toward Copper Adaptation

Aleeza C. Gerstein, Jasmine Ono, Dara S. Lo, Marcus L. Campbell, Anastasia Kuzmin, and Sarah P. Otto

DOI: 10.1534/genetics.114.171124

Supplementary Information for:

"Too much of a good thing: The unique and repeated paths toward copper adaptation"

Gerstein et al. (2015) ***Genetics***

File S1

SUPPLEMENTARY METHODS

Quantitative real-time PCR (qPCR) – To test whether levels of *CUP1* inferred from *in silico* qPCR were consistent with levels of *CUP1* transcription, we assayed RNA levels using quantitative real-time PCR (qPCR). We chose 10 CBM lines that spanned the range of *CUP1* copy number (from lowest to highest): CBM16, CBM22, CBM24, CBM37, CBM2, CBM14, CBM51, CBM4, CBM34, and CBM13. For each line and BY4741, culture was struck from frozen onto a YPD plate and grown at 30°C for 48h. A single colony of each CBM line and two colonies of BY4741 were inoculated into 1mL YPD + 5.5mM copper (a lower concentration was used to allow growth of all lines, including BY4741) and grown for 12 hours at 30°C with shaking, at which point RNA was isolated using the RNEasy Mini Kit from Qiagen, following the yeast protocol. cDNA was reverse transcribed from 500ng of RNA using MultiScribe reverse transcriptase (Life Technologies) and oligo d(T) primers.

Oligonucleotides for qPCR (Table 2) were designed using Primer Express (ABI). mRNA levels of *TAF10* were used for normalization because *TAF10* has stable expression across strains and conditions (TESTE *et al.* 2009). cDNA was diluted 100-fold for *CUP1*, but not *TAF10*, to account for differences in their abundance in the samples. All qPCR reactions were performed using an ABI7000 sequence detection system (Applied Biosystems, Inc.). The reaction volume was 22μL containing 10pmol of each primer and 2μL of each sample with 10μL of 2X SYBR Green Master Mix (Applied Biosystems Inc.). Reaction conditions were 1 cycle of 50°C for 2 min., 1 cycle of 94°C for 10 min., and 40 cycles of 95°C for 15 sec., 60°C for 1 min.

To generate standard curves against which cDNA concentrations could be measured, we obtained cDNA from BY4741, which was then diluted five times, each time using a five-fold dilution, followed by qPCR using the primers for *TAF10* and *CUP1*. Standard curves for BY4741 were plotted such that a 1:1 relationship between fluorescence and sample concentration yields an expected slope of $log_2(10) = -3.32$. All standard curves fit the data well (r^2 >0.99), with slopes between -3.1 and -3.3. *TAF10* and *CUP1* expression levels for every other strain were then measured against their respective standard curves, and then *CUP1* levels were divided by *TAF10* levels to control for variation among samples in total cDNA concentrations. All qPCR experiments were performed with two technical replicates.

Tetrad analyses – To separate the effects of single mutations from other mutations present in the evolved lines (including extra copies of *CUP1*), we crossed all of the CBM lines with BY4739 (*MAT*α *leu2*$\triangle$*0 lys2*$\triangle$*0 ura3*$\triangle$*0*), which has a common genotype yet opposite mating type and different auxotrophies than BY4741, the progenitor of our lines. Cells of both mating types were allowed time to mate overnight on a YPD plate before being struck onto plates lacking histidine and lysine, selecting for diploids. Single colonies were then struck onto selection plates a second time to ensure they were diploids. Culture was taken directly from these plates and frozen in 15% glycerol.

To isolate single mutations, we attempted to sporulate the CBM$\times$BY4739 lines that contained each common mutation or aneuploidy and the fewest number of additional mutations ($\sim$1/3 of the lines). We encountered substantial difficulties in obtaining tetrads from our strains; BY4741, a derivative of S288c, is known to be a poor sporulator (DEUTSCHBAUER and DAVIS 2005; BEN-ARI *et al.* 2006). With a subset of the lines, we attempted to maximize sporulation rates using a variety of different protocols including all combinations of YPD, 1% YPA or 6% YEPD for pre-sporulation, liquid or plates, and PSP2, 1% KAc, or CSHSPO as the sporulation medium, all in liquid (see ELROD *et al.* 2009 for media details). Most combinations were tried at 30°C, but the CSHSPO combinations were also attempted at 25°C and 37°C. In all cases, frozen culture was struck onto YPD plates and grown for 48 hours at 30°C to isolate a single colony for sporulation. Ultimately, we obtained the most success using YPD liquid as a pre-sporulation medium followed by washing 100μL of overnight culture with dH_2O and then plating on 1% KAc at 20°C or 25°C for up to 30 days. Unfortunately, however, we remained unable to sporulate the majority of lines. In particular, despite many attempts, no tetrads were obtained for CBM16 (*PMA1* mutation plus chrII aneuploidy), CBM26 (*PMA1* mutation plus chrI, chrV and chrVIII aneuploidy), CBM29 (*PMA1* mutation plus chrII aneuploidy), CBM47 (*VTC1* mutation), or CBM55 (no mutation identified other than extra copies of *CUP1*).

We were able to sporule CBM2 (chrII aneuploidy), CBM14 (*MAM3* mutation), CBM25 (*MLP1* and *ENA5* mutations), and CBM34 (*VTC4* mutation). CBM25 was not initially chosen for tetrad dissection but was dissected as a contaminate of CBM22 (*VTC1* plus chrVIII and chrXVI aneuploidy), as detected by subsequent sequencing. CBM25 contaminating cells were likely positively selected during the sporulation procedure given that the aneuploid lines in our experiment, like CBM22, had very low sporulation rates. The resulting tetrads were dissected by micromanipulation on YPD plates. The spores were allowed to germinate and grow at 30°C for 3 days before each dissection plate was replica plated to test for mating types and auxotrophies. All tetrads were verified for 2:2 segregation of auxotrophies (except the aneuploid CBM2 - see below) and mating type. Once confirmed, the colonies obtained from each spore were frozen in 15% glycerol. We numbered the dissected tetrads (t1 up to t11) and lettered each haploid spore (a-d).

The genotype of resulting spores was then determined. For CBM14 tetrad lines, *MAM3* was amplified by PCR (primers in Table2), and the product was digested with EcoRV (Fermentas), which specifically cuts the mutant allele at GATATC. The results (one band versus two) were visualized on a 2% agarose gel. CBM25 spores were sequenced on Illumina HiSeq 2000, which is when the strain was discovered to be CBM25 (bearing a mutation in *MLP1* and *ENA5*),

not CBM22. For CBM34 spores, *VTC4* was PCR amplified (Table2) from genomic DNA and the fragment was Sanger sequenced using the forward primer and aligned to the reference sequence using ClustalW at EMBL-EBI (LARKIN *et al.* 2007). All SNPs showed the expected 2:2 segregation pattern.

The segregation pattern for the additional copy of chrII in CBM2 spores was determined for three of the tetrads (t1, t2 and t5) by the presence of the *LYS2* alleles, as detected by PCR. The *LYS2* gene is located on chrII, and the mated diploid from CBM2 carried two functioning copies of the gene (from CBM2) and one copy of the lys2$\triangle$0 allele (from BY4739). Primers were designed to flank the *LYS2* gene. The forward primer was designed 538bp upstream of the start site and the reverse primer was designed 487bp downstream of the stop codon in order to easily detect the deletion by band size (full gene = 5199bp, deletion allele = 708bp) (primers in Table2). For t1 and t2, the two functional copies were inferred to be in the same cell due to the 2:2 segregation of the deletion and wild type alleles. For t5, one functional allele had segregated to each cell and the two aneuploid cells were determined based on PCR detection of the presence of the deletion. Corresponding phenotypes were verified by plating on medium lacking lysine. The segregation pattern for the additional copy of chrII in t3 was determined by Illumina sequencing, followed by calculating the total depth of coverage for each chromosome, as described above.

Southern blots with *CUP1* specific probes were performed to quantify the segregation patterns of *CUP1* among the spores. DNA concentration of genomic DNA isolated from each analyzed spore was measured in triplicate with the Qubit fluorometer (Invitrogen). Based on the average concentration, $2\mu g$ of each sample was loaded into a 1% agarose gel and run at 120V. DNA in the gel was denatured in a NaOH buffer and transferred to a nylon membrane (Hybond N+, GE Healthcare) using capillary transfer in 20x SSC buffer, affixing the DNA to the membrane by baking at 80°C for 2 hours. The membrane was incubated overnight at 57°C, with two biotin labelled probes (Table2). The membrane was then washed in 2x SSC + 0.1% SDS buffer at 56°C 3 times for 15min. Probe binding was visualized using the North2South chemiluminescent detection kit (Thermo Scientific). Blots were exposed onto CL-XPosure Film (Thermo Scientific) for 30sec. to 1min. and developed in a Kodak X-ray film processor. We isolated genomic DNA and ran a Southern blot on three separate occasions for each spore. Controls (BY4741, BY4739, original CBM line) were always run in duplicate on the same gel as related spores. Band intensity was quantified in ImageJ (ABRAMOFF *et al.* 2004) using the “background corrected density" macro (http://rsb.info.nih.gov/ij/macros/BackgroundCorrectedDensity.txt).

LITERATURE CITED

ABRAMOFF, M., P. MAGALHAES, and S. RAM, 2004 Image processing with ImageJ. Biophotonics International **11**: 36–42.

BEN-ARI, G., D. ZENVIRTH, A. SHERMAN, L. DAVID, M. KLUTSTEIN, *et al.*, 2006 Four linked genes participate in controlling sporulation efficiency in budding yeast. PLoS Genet. **2**: e195.

DEUTSCHBAUER, A. M., and R. W. DAVIS, 2005 Quantitative trait loci mapped to single-nucleotide resolution in yeast. Nat. Genet. **37**: 1333–1340.

ELROD, S., S. CHEN, K. SCHWARTZ, and E. SHUSTER, 2009 Optimizing sporulation conditions for different *Saccharomyces cerevisiae* strain backgrounds. In S. Keeney, editor, *Meiosis*, volume 557 of *Methods in Molecular Biology*. Humana Press, 21–26.

GERSTEIN, A. C., D. S. LO, and S. P. OTTO, 2012 Parallel genetic changes and non-parallel gene-environment interactions underlie drug resistance in yeast. Genetics **192**: 241–252.

LARKIN, M. A., G. BLACKSHIELDS, N. BROWN, R. CHENNA, P. A. MCGETTIGAN, *et al.*, 2007 Clustal W and Clustal X version 2.0. Bioinformatics **23**: 2947–2948.

TESTE, M.-A., M. DUQUENNE, J. M. FRANCOIS, and J.-L. PARROU, 2009 Validation of reference genes for quantitative expression analysis by real-time RT-PCR in *Saccharomyces cerevisiae*. BMC Mol. Biol. **10**: 99.

Table S1: Date of isolation for CBM lines. 56 putative mutation lines were isolated from three deep-well boxes (A-C) following exposure to copper (started on 19 Jan 2011). Culture from each well showing growth was streaked onto a YPD plate and assessed for colony size. Eight colonies were randomly chosen from all lines that grew normally on the YPD plates and assayed for growth in copper12. A single copper-resistant colony was chosen from each of the 34 remaining putative mutation lines. All lines were subsequently streaked onto YPG plates to assay respiratory capacity.

Date of isolation	CBM Line	Box	copper12 growth (# of 8)	YPG growth
27 Jan 2011	CBM1	A	7	✓
27 Jan 2011	CBM2	B	6	✓
27 Jan 2011	CBM3	B	3	✓
27 Jan 2011	CBM4	B	7	✓
27 Jan 2011	CBM5	C	5	✓
28 Jan 2011	CBM6	A	4	✓
28 Jan 2011	CBM7	A	6	✓
28 Jan 2011	CBM8	A	0†	petite
28 Jan 2011	CBM9	B	-‡	✓
28 Jan 2011	CBM10	B	-	petite
28 Jan 2011	CBM11	B	8	✓
28 Jan 2011	CBM12	B	-	petite
28 Jan 2011	CBM13	B	8	✓
28 Jan 2011	CBM14	C	7	✓
28 Jan 2011	CBM15	C	-	petite
28 Jan 2011	CBM16	C	7*	petite
28 Jan 2011	CBM17	C	6	✓
28 Jan 2011	CBM18	C	7	✓
29 Jan 2011	CBM19	A	-	petite
29 Jan 2011	CBM20	B	8*	petite
29 Jan 2011	CBM21	B	7	✓
29 Jan 2011	CBM22	C	6	✓
29 Jan 2011	CBM23	C	no growth on YPD	-
29 Jan 2011	CBM24	C	8	✓
30 Jan 2011	CBM25	A	4	✓
30 Jan 2011	CBM26	A	6	✓
30 Jan 2011	CBM27	A	-‡	✓
30 Jan 2011	CBM28	A	-‡	✓
30 Jan 2011	CBM29	A	8*	petite
30 Jan 2011	CBM30	B	5	✓
30 Jan 2011	CBM31	B	-	petite
31 Jan 2011	CBM32	B	-	petite
31 Jan 2011	CBM33	B	8	✓
31 Jan 2011	CBM34	B	8	✓
31 Jan 2011	CBM35	B	0	✓
31 Jan 2011	CBM36	B	8	✓
31 Jan 2011	CBM37	B	8	✓
31 Jan 2011	CBM38	C	-	petite
31 Jan 2011	CBM39	C	0	✓
2 Feb 2011	CBM40	A	-	petite
2 Feb 2011	CBM41	A	0	✓
2 Feb 2011	CBM42	A	-	petite
2 Feb 2011	CBM43	A	-	petite
2 Feb 2011	CBM44	B	8	✓
2 Feb 2011	CBM45	B	8	✓
3 Feb 2011	CBM46	A	4	✓
3 Feb 2011	CBM47	A	7	✓
3 Feb 2011	CBM48	A	-	petite
3 Feb 2011	CBM49	B	8	✓
3 Feb 2011	CBM50	B	0	✓
3 Feb 2011	CBM51	B	5	✓
3 Feb 2011	CBM52	B	0	✓
3 Feb 2011	CBM53	B	6	✓
3 Feb 2011	CBM54	B	3	✓
3 Feb 2011	CBM55	B	4	✓
3 Feb 2011	CBM56	C	no growth on YPD	-

* These lines were included in our study because colonies were not noticeably petite on YPD. Whole-genome sequencing indicated very little depth of coverage for mitochondrial genes for the copper resistant colonies analysed. These were subsequently shown to be incapable of growth on YPG plates (respiration deficient).

† Because colonies on YPD plates were not noticeably petite, this line was assayed for copper tolerance. As none of the 8 colonies grew, this line was dropped.

‡ These colonies were small on YPD but later shown to be capable of respiration (growth on YPG). Whole-genome sequencing was then conducted to determine the genetic basis of copper resistance.

Table S2: T-test results comparing maximum growth rates of the CBM lines to growth of BY4741 in YPD + ferric citrate. Maximum growth rates were highly correlated among iron concentrations (10mM vs 40mM: $r = 0.89$, $t = 11.00$, $df = 31$, $p < 0.001$; 60mM vs 40mM: $r = 0.56$, $t = 3.72$, $df = 31$, $p = 0.0008$), so only 40mM results are presented in the text. Growth was assayed by automated OD readings over a 24 period in the Bioscreen C.

	10 mM ferric citrate			**40 mM ferric citrate**			**60 mM ferric citrate**		
Line	t	df	*p*-value	t	df	*p*-value	t	df	*p*-value
CBM1	-0.14	6.09	0.89	-0.34	7.80	0.74	-0.83	6.35	0.44
CBM2	-1.23	4.64	0.28	-5.47	6.78	0.001	1.8	4.83	0.13
CBM3	-0.04	5.75	0.97	-7.01	7.81	0.0001	2.81	6.6	0.03
CBM4	1.03	6.97	0.34	-2.16	5.43	0.078	0.32	6.23	0.76
CBM5	-1.86	4.69	0.13	-0.03	6.16	0.98	0.89	11.04	0.39
CBM6	-4.09	6.01	0.01	-8.48	5.86	0.0002	-2.59	9.58	0.03
CBM7	-10.42	5.64	0	-12.66	5.49	< 0.0001	-0.67	6.12	0.53
CBM11	-0.58	5.26	0.59	-9.81	4.99	0.0002	3.27	5.79	0.02
CBM13	-0.19	7.99	0.86	-0.22	5.80	0.83	1.89	4.67	0.12
CBM14	2.51	7.27	0.04	-0.0001	5.23	1.00	1.42	4.69	0.22
CBM16	-2.76	7.88	0.03	-27.41	7.61	< 0.0001	-2.58	8.05	0.03
CBM17	-8.88	4.52	0	-16.51	7.24	< 0.0001	-4.86	18.19	0
CBM18	-1.41	4.85	0.22	-3.42	6.07	0.01	1.31	4.5	0.25
CBM20	-6.3	4.42	0	-33.61	4.64	< 0.0001	-2.1	6.95	0.07
CBM21	-9.09	4.96	0	-11.87	9.00	< 0.0001	0.29	6.68	0.78
CBM22	-2.85	7.91	0.02	-11.10	5.11	0.0001	-3.74	8.64	0
CBM24	1.32	4.79	0.25	-1.17	5.32	0.29	0.34	6.71	0.75
CBM25	0.5	7.28	0.63	3.67	5.19	0.01	1.24	25	0.23
CBM26	-15.22	7.59	0	-36.20	5.11	< 0.0001	-3.01	12.37	0.01
CBM29	-4.92	7.69	0	-28.54	7.87	< 0.0001	-1.91	18.92	0.07
CBM30	-0.41	5.85	0.7	-6.37	7.97	0.0002	4.36	6.03	0
CBM33	-1.28	7.96	0.24	-1.49	4.83	0.20	1.59	6.38	0.16
CBM34	-3.07	7.92	0.02	-2.14	5.72	0.08	1.45	6.84	0.19
CBM36	-1.42	6.01	0.21	0.26	5.31	0.81	0.01	5.78	1
CBM37	0.06	5.45	0.96	-0.38	5.22	0.72	-1.37	8.43	0.21
CBM45	-0.26	5.69	0.8	-0.13	5.10	0.90	1.31	6.04	0.24
CBM46	-0.3	7.67	0.77	-0.90	4.69	0.41	0.89	6.23	0.41
CBM47	0.05	5.99	0.96	-0.82	4.95	0.45	2.45	13.5	0.03
CBM49	-11.04	4.48	0	-7.83	4.72	0.0007	-0.38	5.16	0.72
CBM51	0.44	7.68	0.67	-0.21	5.74	0.84	0.52	10.86	0.61
CBM53	-0.01	7.97	0.99	-0.93	5.36	0.39	0.44	5.54	0.68
CBM54	0.14	7.6	0.89	1.18	7.28	0.27	1.09	6.95	0.31
CBM55	1.38	4.5	0.23	1.54	7.84	0.16	2.12	7.33	0.07

Table S3: Predicted transcription factor binding site gains and losses from intergenic mutations. The nearest ORFs upstream (5' on the Watson strand) or downstream (3') are given, as well as the distances to the start sites (brackets) and the orientation of the binding site (S: binding site precedes start of ORF; E: binding site after end of ORF). In bold are binding sites within 500 bp of the start of a gene on the coding strand. Neighbouring repeat elements, multi-copy tRNAs, or dubious ORFs were ignored.

Line	Position	Upstream ORF	Downstream ORF	Mutation	TF lost	TF gained
CBM1	XVI.420661	**YPL071C [143] (S)**	***MUK1* [287] (S)**	A>T	n/a	n/a
CBM3	VII.150650	***COX4* [479] (S)**	*TPN1* [2126] (E)	G>T	*FKH2*, *FKH1*, *HCM1*	*ORC2*, *SFP1*, *SPT15*
CBM5	XIV.284255	YNL190W [1860] (E)	***SRP1* [5] (S)**	T>G	*FKH2*, *HCM1*, *SUM1* *NHP6A*, *NHP6B*, *ORC2* *PHO2*, *SMP1*, *SPT15*, *YAP1*	n/a
CMB5,13,21	X.654261	**YJR124C [23] (S)**	*ENT3* [1702] (E)	T>C	*SUM1*, *ORC2*, *STB3*	n/a
CBM7	III.306327	YCR102C [860] (S)	*PAU3* [1474] (S)	G>T	n/a	*GAT1*, *GLN3*
CBM7	IX.370383	***PAN1* [475] (S)**	**YIR007W [321] (S)**	C>G	n/a	*GAT1*, *GLN3*, *GZF3*, *ECM23*, *SRD1*
CBM11	XII.605283	***CDC42* [496] (S)**	*BNA5* [1836] (E)	1D indel	n/a	*ORC2*, *SFP1*, *YGR067C*
CBM24	IV.805517	*SEC7* [3295] (S)	*HSP42* [1104] (S)	G>A	*STP4*	*UME6*
CBM24	IV.805485	*SEC7* [3263] (S)	*HSP42* [1136] (S)	A>G	*LYS14*, *YKL222C*, *YRR1*	*AR080*, *CEP3*, *PUT3*, *RDS2*, *TBS1*
CBM29	XV.566240	***ADE2* [49] (S)**	*AFI1* [3318] (E)	G>C	*RAP1*	n/a
CBM29	VII.1376	(telomere)	*COS12* [1414] (S)	A>C	*NHP6B*, *NHP6A*, *ORC2* *PHO2*, *SPT15*, *YOX1*	n/a
CBM34	XI.364516	*PTM1* [1894] (S)	*SNR69* [260] (S)	complex 1I indel	n/a	*GAT1*, *GLN3*, *GZF3*, *NHP6B*, *PHO2*, *SFP1*
CBM49	V.438349	YER134C [546] (S)	*GDI1* [1267] (S)	G>C	*SKN7*	n/a
CBM49	XIII.420239	***PDS5* [210] (S)**	*VPS20* [1910] (E)	A>C	*DOT6*	*ERT1*
CBM51	IV.310552	***RPP1A* [430] (S)**	*THI3* [1919] (E)	A>G	*FKH2*, *HCM1*, *NHP6A*, *NHP6B*, *PHO2*, *SPT15*	*ORC2*, *SUM1*

Table S4: T-test results comparing maximum growth rate in copper8 between CBM lines and BY4741. Growth was assayed by automated OD readings over a 24 hour period in the Bioscreen C.

	Maximum growth rate		
Line	t	df	p-value
CBM1	13.65	25.16	< 0.0001
CBM2	11.41	24.19	< 0.0001
CBM3	10.60	25.60	< 0.0001
CBM4	9.32	25.73	< 0.0001
CBM5	14.47	24.05	< 0.0001
CBM6	13.25	24.39	< 0.0001
CBM7	8.80	24.11	< 0.0001
CBM11	12.78	24.79	< 0.0001
CBM13	14.36	24.56	< 0.0001
CBM14	11.09	25.54	< 0.0001
CBM16	11.44	24.71	< 0.0001
CBM17	12.09	24.68	< 0.0001
CBM18	15.29	25.43	< 0.0001
CBM20	11.56	24.36	< 0.0001
CBM21	8.12	24.19	< 0.0001
CBM22	12.21	25.66	< 0.0001
CBM24	0.43	5.49	0.68
CBM25	9.93	25.85	< 0.001
CBM26	3.81	27.14	0.0007
CBM28	6.73	25.66	< 0.0001
CBM29	11.02	24.65	< 0.0001
CBM30	10.72	25.89	< 0.0001
CBM33	14.71	24.24	< 0.0001
CBM34	11.10	26.13	< 0.0001
CBM36	12.53	21.12	< 0.0001
CBM37	14.89	27.70	< 0.0001
CBM44	14.02	26.02	< 0.0001
CBM45	13.05	25.99	< 0.0001
CBM46	13.78	26.47	< 0.0001
CBM47	14.37	27.20	< 0.0001
CBM49	7.88	26.01	< 0.0001
CBM51	7.32	25.05	< 0.0001
CBM53	10.24	25.84	< 0.0001
CBM54	4.54	24.60	0.0001
CBM55	11.30	26.39	< 0.0001

Table S5: T-test results comparing maximum growth rate in YPD between CBM lines and BY4741. Growth was assayed by automated OD readings over a 24 hour period in the Bioscreen C.

	Maximum growth rate		
Line	t	df	*p*-value
CBM1	-2.62	27.98	0.014
CBM2	-1.50	6.89	0.18
CBM3	-4.72	26.93	<0.0001
CBM4	0.90	5.96	0.40
CBM5	-1.44	18.46	0.17
CBM6	-5.86	26.06	<0.0001
CBM7	-2.20	5.95	0.07
CBM11	-3.86	14.88	0.002
CBM13	-2.31	27.00	0.028
CBM14	0.0004	7.30	1.00
CBM16	-6.69	25.79	<0.0001
CBM17	-8.63	26.77	<0.0001
CBM18	-0.66	7.18	0.53
CBM20	-0.48	5.34	0.65
CBM21	-0.22	5.02	0.84
CBM22	-8.88	26.52	<0.0001
CBM24	1.86	8.33	0.10
CBM25	1.69	6.10	0.14
CBM26	-19.28	26.76	<0.0001
CBM28	-7.63	24.87	<0.0001
CBM29	0.24	5.65	0.82
CBM30	-1.80	6.04	0.12
CBM33	-1.63	9.12	0.14
CBM34	-3.89	26.23	0.0006
CBM36	-5.19	24.35	<0.0001
CBM37	-1.54	6.94	0.17
CBM44	-1.50	9.98	0.17
CBM45	-4.23	26.70	0.0002
CBM46	-4.47	25.03	0.0001
CBM47	-1.51	9.90	0.16
CBM49	-9.68	25.53	<0.0001
CBM51	0.20	6.21	0.85
CBM53	0.30	9.01	0.77
CBM54	0.46	6.10	0.66
CBM55	1.96	5.78	0.10

Table S6: T-test results comparing maximum growth rate in YPG between CBM lines and BY4741. Growth was assayed by automated OD readings over a 24 hour period in the Bioscreen C.

	Maximum growth rate		
Line	t	df	*p*-value
CBM1	0.25	13.04	0.81
CBM2	-5.33	16.19	0.0001
CBM3	-6.68	18.30	< 0.0001
CBM4	1.01	17.52	0.33
CBM5	-0.30	14.22	0.77
CBM6	-56.27	17.09	< 0.0001
CBM7	-5.78	16.03	< 0.0001
CBM11	-8.83	15.96	< 0.0001
CBM13	-1.03	11.74	0.32
CBM14	0.84	13.59	0.42
CBM16	-59.60	18.40	< 0.0001
CBM17	-12.32	12.62	< 0.0001
CBM18	-0.41	21.13	0.69
CBM20	-69.59	24.25	< 0.0001
CBM21	-21.28	13.39	< 0.0001
CBM22	-31.41	20.28	< 0.0001
CBM24	-1.58	23.14	0.13
CBM25	1.94	19.23	0.07
CBM26	-21.35	20.68	< 0.0001
CBM28	-39.78	36.21	< 0.0001
CBM29	-91.71	45.36	< 0.0001
CBM30	-5.56	21.67	< 0.0001
CBM33	-1.64	26.01	0.11
CBM34	-0.75	15.98	0.46
CBM36	-0.20	13.43	0.85
CBM37	-1.33	14.82	0.20
CBM44	-1.71	15.21	0.11
CBM45	-2.14	12.96	0.05
CBM46	-1.04	16.19	0.31
CBM47	-0.35	13.78	0.73
CBM49	-7.57	13.07	< 0.0001
CBM51	0.27	14.87	0.79
CBM53	0.18	13.44	0.86
CBM54	-0.61	13.69	0.55
CBM55	-0.77	18.51	0.45

Table S7: Summary of linear model analyses of the maximum growth rate of tetrads, assayed in YPD within the Bioscreen C. For each line, we show the analysis of a full model accounting for the genes listed below. Thus, CBM2 shows evidence for an effect of an additional copy of chrII on growth in YPD. Significant *p*-values are in bold.

Line	Term	Estimate	t	df	*p*-value
CBM2	*CUP1*	-4.66E-08	-0.48	13	0.64
	+chrII	-7.37E-02	-3.39	13	**0.0048**
CBM14	*CUP1*	8.20E-08	1.60	21	0.12
	MAM3	-3.61E-02	-1.75	21	0.095
CBM25	*CUP1*	2.71E-08	0.62	12	0.54
	MLP1	-2.67E-02	-1.086	12	0.30
	ENA5	5.62E-03	0.26	12	0.80
CBM34	*CUP1*	-1.58E-08	-0.48	21	0.63
	VTC4	2.17E-02	1.29	21	0.21

Table S8: Summary of linear model analyses of the maximum growth rate of tetrads assayed in copper9, after correcting for growth in YPD (maximum growth rate in copper9 minus maximum growth rate in YPD), both measured within the Bioscreen C. For each line, we show the analysis of a full model accounting for the genes listed below. Only CBM2 showed evidence for an effect of a mutation on growth in YPD (see Table **S7**). Significant *p*-values are in bold.

Line	Term	Estimate	t	df	*p*-value
CBM2	*CUP1*	2.96E-07	3.18	13	**0.0072**
	chrII	1.10E-01	5.30	13	**0.00015**
CBM14	*CUP1*	4.40E-08	0.80	21	0.43
	MAM3	5.49E-02	2.48	21	**0.022**
CBM25	*CUP1*	8.50E-08	1.53	12	0.15
	MLP1	2.11E-02	0.67	12	0.51
	ENA5	-5.93E-03	-0.21	12	0.84
CBM34	*CUP1*	1.70E-07	4.12	21	**0.00049**
	VTC4	3.48E-02	1.65	21	0.11

Table S9: Additional mutations identified in the small-colony forming CBM lines. *CUP1* coverage for each line is provided in the second column and does not account for additional copies via chrVIII aneuploidy.

CBM line	*CUP1* coverage	Genome Position (chr.bp)	Gene	Mutation (Watson strand)	Position (from 5' end)	Amino acid change	Exchangeability
CBM9	0.69	VII.481622	*PMA1*[a]	C>T	1045	Gly>Ser	0.304
CBM27	0.83	VII.482121	*PMA1*	3D indel (AAC/—)	544	Val> −	
		mito.83071	intergenic	A>G			
CBM28	1.25	IV.43829&IV.43830	intergenic	CA>AT			
		chrIII aneuploidy					
		chrV aneuploidy					
		chrVIII aneuploidy					

[a] As a sample from the population was sequenced, this mutation was not fixed but was called as a "heterozygote" (43.4% of reads).

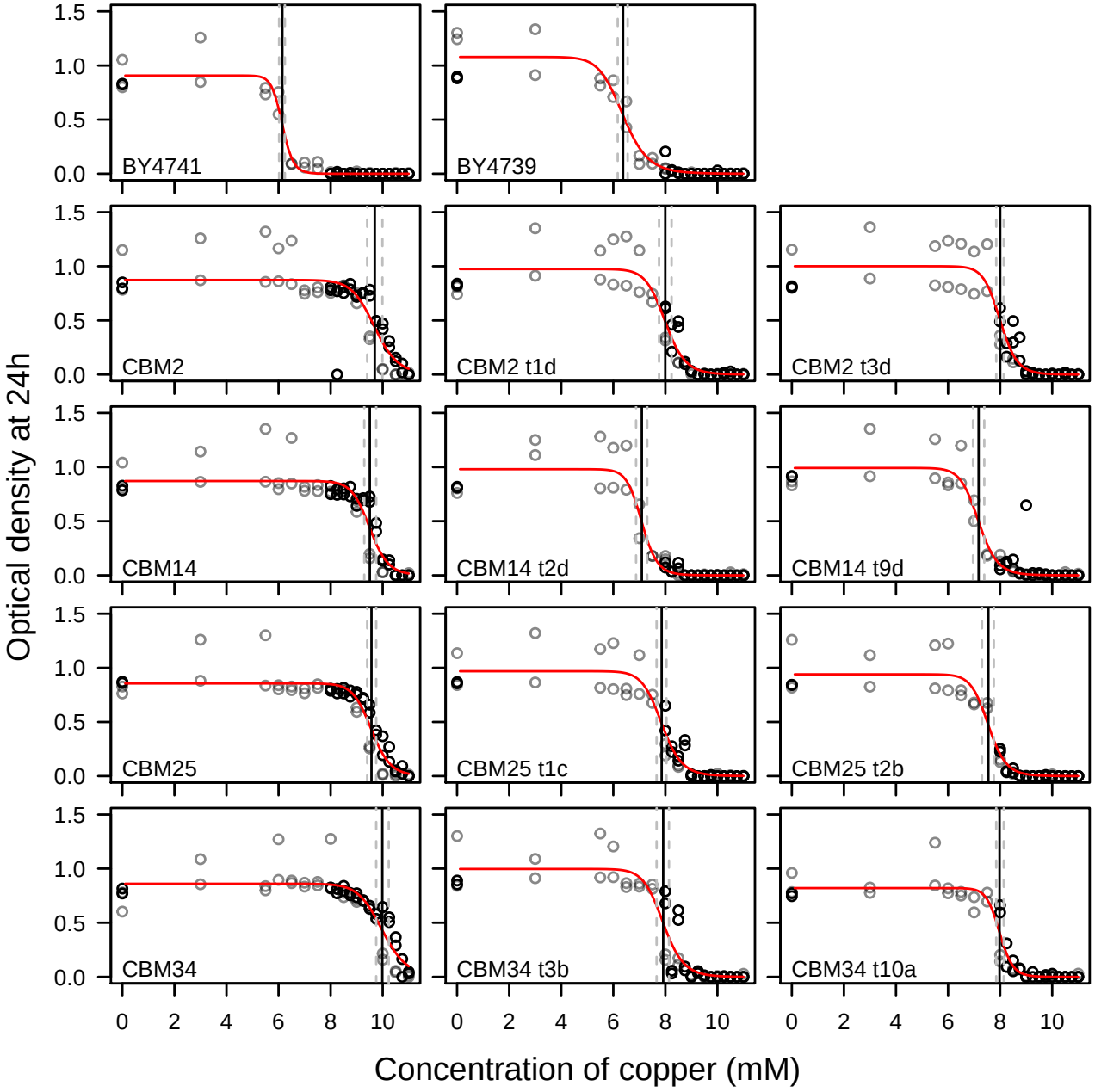

Figure S1: Optical density after 24 hours of growth in the Bioscreen C for specific spores over a range of copper concentrations. Spores were chosen that had lower *CUP1* copy number and carried either an extra copy of chrII (CBM2 lines), a SNP in *MAM3* (CBM14 lines), a SNP in *MLP1* (CBM25 lines) or a SNP in *VTC4* (CBM34 lines). Grey and black circles represent data points collected on two separate days, with two replicates per day. Curves drawn in red are maximum likelihood fits using the methods described in GERSTEIN *et al.* (2012), with the estimated IC_{50} represented by a vertical black line and its corresponding 95% confidence interval shown by the grey dashed lines.

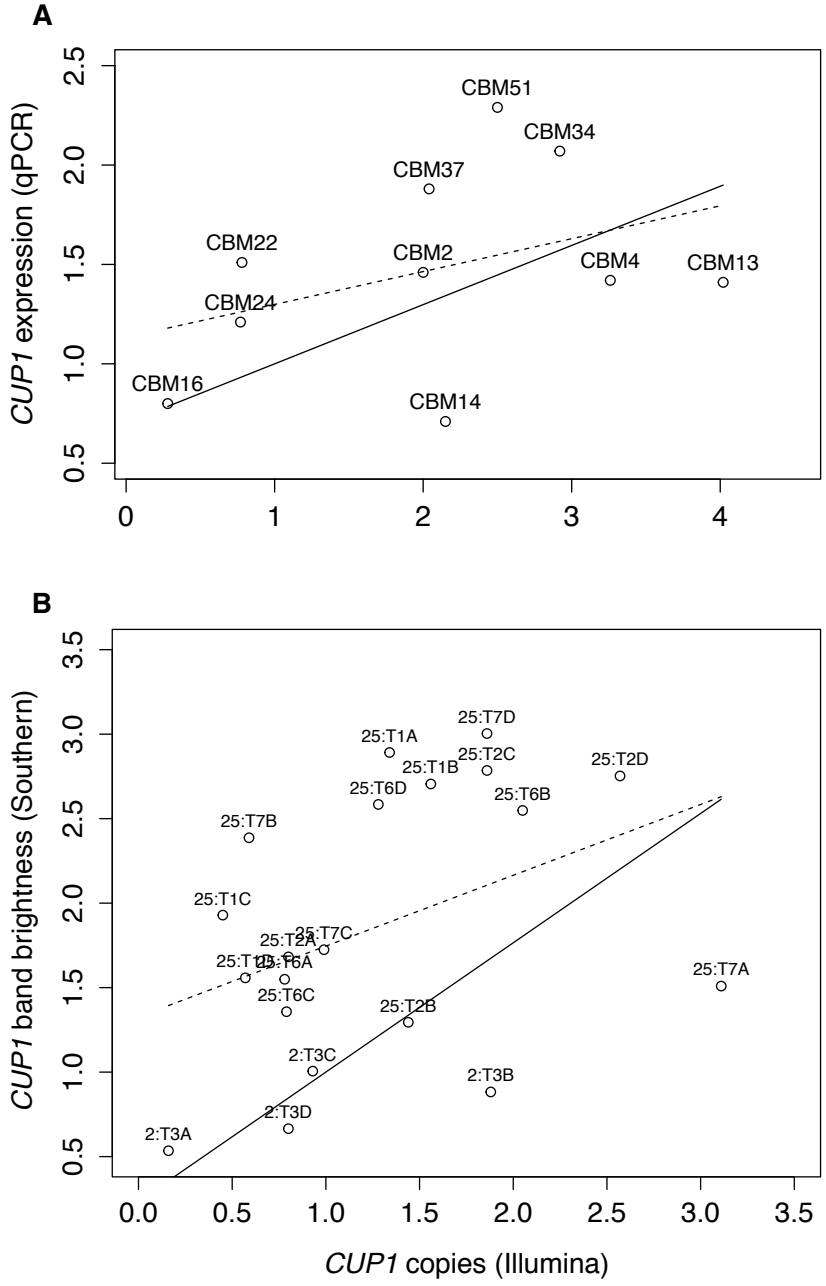

Figure S2: Comparison of *CUP1* copy number assays. A. *CUP1* expression level was determined via qPCR and compared with the *in silico* qPCR estimates based on the fastq Illumina files for ten CBM lines. Expression levels for *CUP1* (normalized to *TAF10*) were obtained by qPCR, with the y-axis giving expression levels relative to the BY4741 ancestral line. The slope is significant when forced through the (1,1) point, which assumes that both axes are scaled to the ancestor (even though the derived BMN lines and not BY4741 were used as the control in the *in silico* qPCR assays; p = 0.02, solid), but the slope is not significant otherwise (p = 0.27, dashed). B. *CUP1* copy number was estimated by band brightness from Southern blots and compared with *in silico* qPCR estimates for the lines established from tetrads. Band brightness from the Southerns was normalized to the average of two BY4739 bands run on the same gels (recall that the CBM lines had been crossed to BY4739 to generate the tetrads; normalizing to the two BY4741 bands yielded similar results). Only those tetrads for which whole-genome sequencing was performed are included (e.g., "25:t1a" refers to "CBM25, tetrad 1, colony a"). The slope is significant when forced through the (1,1) point (p = 0.02; solid) and marginally significant otherwise (p = 0.08, dashed).

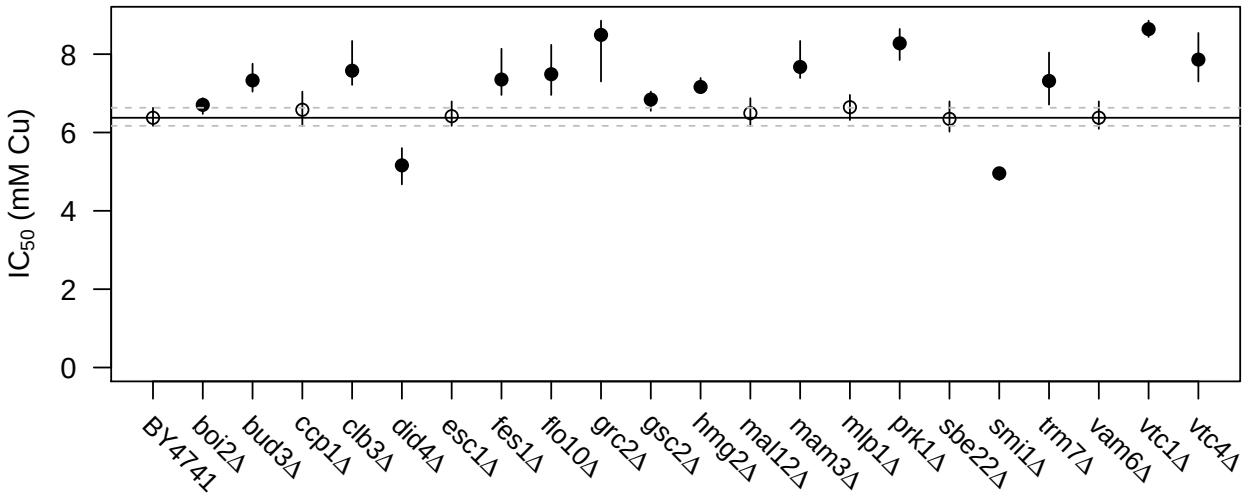

Figure S3: Copper tolerance of *S. cerevisiae* knockout lines for genes identified in our experiment. Solid circles identify lines that have significantly different tolerance than BY4741, measured as IC_{50} (bars represent 95% confidence intervals). The horizontal lines are for illustrative purposes to indicate the mean (solid line) and confidence interval (dashed lines) for BY4741.

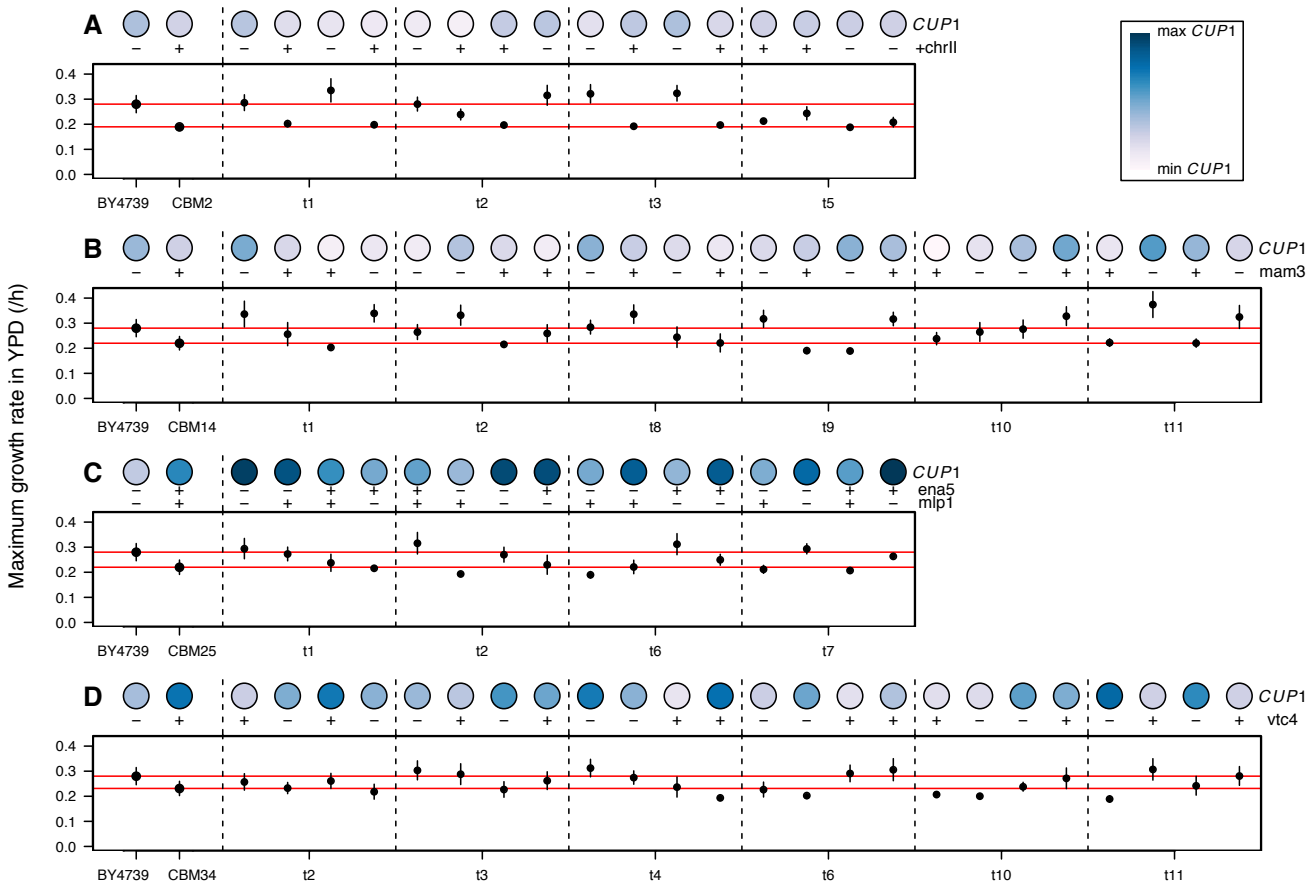

Figure S4: Maximum growth rate of tetrads in YPD, as measured by the Bioscreen C. Tetrads were derived from four different CBM lines: A. CBM2, B. CBM14, C. CBM25, and D. CBM34. For each line, maximum growth rate was assayed within the Bioscreen C on a single day (± 1 SE across replicate wells). The darkness of the circle represents the relative number of copies of *CUP1*, as assayed from Southern blots. Presence ($+$) or absence ($-$) of a segregating mutation is also noted. All lines are compared to the growth rate of the two parents, BY4739, and the relevant CBM parent (red lines), except for the tetrads derived from CBM25 for which parental growth rate was not assayed (due to its initially being considered CBM22, see Materials and Methods).

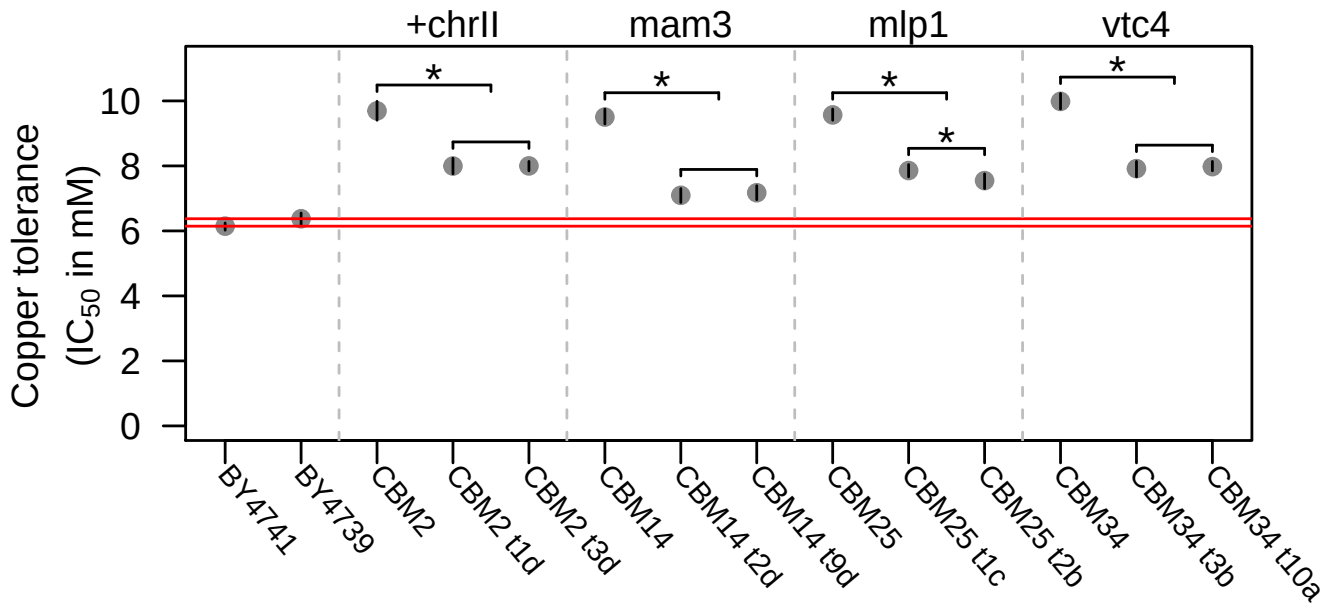

Figure S5: Copper tolerance, as measured by IC_{50} after 24 hours of growth in the Bioscreen C for specific spores. Lines were chosen because they had low *CUP1* copy number and carried either an extra copy of chrII (CBM2 lines), a mutation in *MAM3* (CBM14 lines), a mutation in *MLP1* (CBM25 lines), or a mutation in *VTC4* (CBM34 lines). All mutant lines had a significantly higher IC_{50} than either of the BY controls, and all spores had a significantly lower IC_{50} than their CBM parent. Horizontal bars indicate statistical comparisons, where an asterisk (*) above a bar indicates statistical significance ($p < 0.05$). Among the spores carrying the same allele, only the CBM25 spores differed significantly from one another in IC_{50}, and only marginally so if corrected for multiple comparisons. Note that CBM25 t1c also carries the mutation in *ENA5*. Vertical bars represent 95% confidence intervals.